

# Application of Electronic Personal Dosimeter in Thermo-Luminescence and Isotopic Ratio Dating of Limestone Using Uranium Series

**Tshegofatso Whittington Solomon**  
[orcid.org/0000-0003-0283-3164](https://orcid.org/0000-0003-0283-3164)

Dissertation submitted in *partial* fulfillment of the requirements for the degree of Master of Science in Applied Radiation Science and Technology at the Mafikeng Campus of the North-West University

Supervisor: Prof. Manny Mathuthu

Graduation: October 2017

Student number: 16833058


<http://www.nwu.ac.za/>



**Declaration**

I solemnly declare that this dissertation is my own work. It is submitted for the fulfilment of the requirements of the degree of Master of Science in Applied Radiation Science and Technology at Centre for Applied Radiation Science and Technology (CARST) under the Faculty of Agriculture Science and Technology (FAST) of the North-West University, Mafikeng Campus. This dissertation has not been submitted before at any University. Other sources of information have been noted by means of reference.

LIBRARY	
MAFIKENG CAMPUS	
CALL NO.:	2021 -02- 0 1
ACC.NO.:	
NORTH-WEST UNIVERSITY	



Signed by student.....

**Tshegofatso Whittington Solomon**

...11 December 2016...

**Date**



Signature

Singed by Supervisor .....

**Prof Manny Mathuthu**

12 December 2016...

**Date**

## Abstract

Application of electronic personal dosimeter in Thermo-Luminescence and isotopic ratio dating of limestone using uranium series has been examined in the dating of prehistoric activities in Gaborone area of Mogoditshane-Tsolamosese (Block 4) Botswana. Isotopic ratio of the stable  $^{206}\text{Pb}$  to the parent nuclide  $^{238}\text{U}$ , was valuable to this research as it enabled the isotopic ratio technique to be applied for the study with better precision and accuracy.

The aim of this research was to investigate the age of limestone existence by Thermo-Luminescence (TL) and isotopic ratio dating of limestone using uranium series measured by electronic personal dosimeter (EPD). This was achieved by quantifying the limestone sediments used in Gaborone at different topographic locations as affected by natural and human activities, and thus determining the effectiveness of Thermo-Luminescence and isotopic ratio methods on dating of limestone. From both Thermo-Luminescence and isotopic ratio methods, varying results were obtained with average limestone ages of 26 MY and 16 MY respectively for the Gaborone area of Mogoditshane-Tsolamosese. The results of this work revealed that the isotopic ratio technique is more reliable than EPD-TL for limestone dating, and thus the  $^{207}\text{Pb}/^{206}\text{Pb}$  inverse Concordia plot from Isoplot gave a weighted mean age of the samples as  $4308 \pm 1900/-770$  MY, with an MSWD of 0.51.

## **Acknowledgements**

Special thanks go to my supervisor Prof. Manny Mathuthu for his support and guidance on this work. It was because of his humility, humbleness and patience that this work is a success. I would also like to thank the Centre for Applied Radiation Science and Technology (CARST) management for giving me the opportunity to be their student.

I also acknowledge the Chief Technician Ms. Mpho Tsheole who helped me with the ICP-MS sample analysis and CASRT students who helped me with the research.

I am also indebted to my family, friends and colleagues for their encouragement throughout my studies, I bow before all of these people and humbly pray that the Lord Jesus Christ, Son of God almighty abundantly bless the lives of these people who have been part of this work.

## LIST OF ABBREVIATIONS AND ACRONYMS

BIFs:	Banded Ironstone Formations
CaCO <sub>3</sub> :	Calcium Carbonate (Calcite)
cpa	Counts per year
cps	Counts per second
DR:	Dose Rate
EPD:	Electronic Personal Dosimeter
ERD:	Equivalent Radiation Dose
ESR:	Electron Spin Resonance
ICP-MS	Inductively Coupled Plasma Mass Spectrometer
ID:	Identity
IRSL	Infrared Stimulated Luminescence
IsR:	Isotopic Ratio
MY:	Million years
NTGB:	Neoproterozoic Tati Greenstone Belt
OSL:	Optically Stimulated Luminescence
SAR:	Single-Aliquot Regenerative-dose
TL:	Thermo-Luminescence
UV:	Ultraviolet
α:	Alpha
β:	Beta
γ:	Gamma

## LIST OF FIGURES

Figure 1: The root of U-series dating via the activity ratio of $^{230}\text{Th} / ^{234}\text{U}$ (Bangert, 1980).....	11
Figure 2: The full $^{238}\text{U}$ isotope decay chain (Reynolds, 2015) .....	13
Figure 3a: The time dependent change of activity ratios of $^{230}\text{Th} / ^{234}\text{U}$ starting from different initial $^{234}\text{U} / ^{238}\text{U}$ ratios ( $r_0$ ) (Bangert, 1980).....	14
Figure 3b: A plot of the relationship between $^{234}\text{U} / ^{238}\text{U}$ and age of a sample (Stanley, 2012) .....	15
Figure 4: Chemical separation procedure for U and Thorium (Duval, 2016) .....	17
Figure 5: Alpha Spectra of U and Th Isotopes (Bangert, 1980).....	18
Figure 6a: Map of Gaborone showing GPS locations of sample collection. ....	23
Figure 6b: GPS locations of sample collection. ....	24
Figure 7: The 6600 Harshaw TLD reader (LHS) and the Thermo-Luminescence dosimeter (TLD 0011) (RHS) with positions iii) and iv) covered with the sample aliquots .....	32
Figure 8: Bar chart representation of sample doses from the TLD results .....	33
Figure 9: Bar chart representation of EPD-RADEYE results analysis for sample doses .....	34
Figure 10: EPD dating results of Limestone sample ages .....	63
Figure 11: Bar chart representation of isotopic ratio dating results of Limestone sample ages .....	64
Figure 12: Inverse U-Pb Concordia for the limestone samples. ....	65

## LIST OF TABLES

Table 1: Principal parent and daughter isotopes used in radiometric dating .....	3
Table: 2. GPS coordinates of the sample sites.....	22
Table 3: NexION 300q ICP-MS Instrumental Parameters (Bosnak, 2014).....	27
Table 4: TLD results for the sample aliquots, done on 27/11/2015.....	31
Table 5: EPD-RADEYE results for the samples analyzed.....	34
Table 6: Nuclide identification report from gamma spectrum analysis for sample A .....	38
Table 7: Nuclide identification report from gamma spectrum analysis for sample B.....	39
Table 10: Nuclide identification report from gamma spectrum analysis for sample E.....	42
Table 11: Nuclide identification report from gamma spectrum analysis for sample F .....	43
Table 12: Nuclide identification report from gamma spectrum analysis for sample G .....	44
Table 13: Nuclide identification report from gamma spectrum analysis for sample H .....	45
Table 14: Nuclide identification report from gamma spectrum analysis for sample I.....	46
Table 15: Nuclide identification report from gamma spectrum analysis for sample J .....	47
Table 16: Nuclide identification report from gamma spectrum analysis for sample K .....	48
Table 17: Nuclide identification report from gamma spectrum analysis for sample L.....	49
Table 18: Nuclide identification report from gamma spectrum analysis for sample M.....	50
Table 19: Nuclide identification report from gamma spectrum analysis for sample N .....	51
Table 20: Nuclide identification report from gamma spectrum analysis for sample O .....	52
Table 21: Nuclide identification report from gamma spectrum analysis for sample P.....	53
Table 22: Nuclide identification report from gamma spectrum analysis for sample Q .....	54
Table 23: Nuclide identification report from gamma spectrum analysis for sample R .....	55
Table 24: Nuclide identification report from gamma spectrum analysis for sample S .....	56
Table 25: Nuclide identification report from gamma spectrum analysis for sample T.....	57
Table 26: Atomic abundances of samples from the ICP – MS analysis.....	58
Table 27: The Pb isotopic ratios for each Sample ID.....	60
Table 29: Age calculation from the isotopic ratio results for the limestone samples.....	62
Table 30: Concordia data for Isoplot age calculation. ....	65

NWU  
LIBRARY

# Table of Contents

Declaration.....	ii
Abstract.....	iii
Acknowledgements .....	iv
LIST OF ABBREVIATIONS AND ACRONYMS .....	v
LIST OF FIGURES.....	vi
LIST OF TABLES.....	vii
CHAPTER 1: INTRODUCTION AND PROBLEM STATEMENT.....	1
1.1 Introduction .....	1
1.2 Problem Statement.....	3
1.3 Research Aim and Objectives .....	5
1.3.1 Aim .....	5
1.3.2 Specific Objectives .....	5
CHAPTER 2: LITERATURE REVIEW .....	6
2.1 Background.....	6
2.2 Thermoluminescent Dating .....	7
2.3 Benefits and limitations of Thermo-Luminescence.....	20
CHAPTER 3: METHODS AND MATERIALS .....	22
3.1 Geographical location of samples collection site .....	22
3.2 Techniques of radioactive dating .....	24
3.3 TL Emission and Dose Response .....	25
3.4 Thermo-Luminescence and Isotopic Ratio Dating.....	25
3.4.1 Method 1: Electronic Personal Dosimeter (EPD).....	26
3.4.2 Thermo-Luminescence Dosimeters (TLD).....	26

<b>3.5 Method 2: ICP – MS Isotopic Ratio .....</b>	<b>27</b>
<b>3.5.1 Instrumentation .....</b>	<b>27</b>
<b>3.5.2 Interference reduction.....</b>	<b>27</b>
<b>3.5.3 Sample Run .....</b>	<b>28</b>
<b>3.5.4 ICP-MS Trace Calibration for trace element analysis.....</b>	<b>29</b>
<b>CHAPTER 4: RESULTS AND DISCUSSIONS .....</b>	<b>30</b>
<b>4.1 Introduction .....</b>	<b>30</b>
<b>4.2 EPD /TLD (SARA) Technique data .....</b>	<b>31</b>
<b>4.3 Gamma spectrometry results .....</b>	<b>35</b>
<b>4.4 ICP-MS Isotopic Ratio Results .....</b>	<b>58</b>
<b>4.5 Results for age determination due to EPD.....</b>	<b>60</b>
<b>4.6 Results for age determination by ICP – MS isotopic ratio technique .....</b>	<b>61</b>
<b>4.6.1 Age calculation from isotopic abundances .....</b>	<b>61</b>
<b>4.6.2 U-Pb Inverse Concordia.....</b>	<b>64</b>
<b>CHAPTER 5: CONCLUSIONS AND RECOMMENDATIONS.....</b>	<b>67</b>
<b>REFERENCES.....</b>	<b>69</b>
<b>Appendix A: List of publications from this work .....</b>	<b>72</b>

## CHAPTER 1: INTRODUCTION AND PROBLEM STATEMENT

### 1.1 Introduction

Thermo-Luminescence (TL) dating is the phenomenon of determining ages of minerals, natural and human activities that has occurred some years ago, this is done by determining the amount of accumulated dose of radiation for the time that passed by material containing minerals such as lava and limestones was either heated and either sediments exposed to sunlight. When limestone containing materials heat up during measurements a process termed thermo-Luminescence occurs. Limestone is a form of calcareous sedimentary type of rock made up of the calcite mineral. During calcination lime is produced from calcite mineral for commercial use. In its widest explanation the term limestone embraces any calcareous material such as chalk, marble, lime shell, travertine, etc. collectively possessing diverse and distinct physical properties (Aitken, 1985). Calcite and aragonite are crystalline equivalents of limestone (i.e. possessing similar chemical configurations) are. Prehistoric men frequently used limestone caves as their domicile or shelter; and today, many remains of their lives are concealed deep underground by subsequently precipitated calcite formations, and speleothems. Such "speleothems" are usually regarded to be a most suitable material for dating purposes, as they are not easily altered as bone material do after long periods of being concealed.

Uranium series dating seems to be a most reliable and rather frequently used technique to determine the formation age of such speleothems (Aitken, 1985). The application of Thermo-Luminescence technique relies mainly on the sensitivity of natural minerals in bagging the radiation energy from a mixed environmental radiation field and storing it over long periods of time (Prescott and Hutton, 1995). Thermal or sunlight stimulation of the minerals or materials of interest affects a zeroing of the luminescence indication through thermal or optical detrapping of charges from defect sites (Chawla, 1997).



The beginning of present isotopic dating methods (Dalrymple, 2006) has evolved since the discovery of radioactivity by Henri Becquerel in 1896, the isolation of radium by Marie Curie, the discovery of radioactive decay laws in 1902 by Ernest Rutherford and Frederick Soddy, the discovery of isotopes in 1910 by Soddy, and the development of the quantitative mass spectrograph in 1914 by J. J. Thomson (Dalrymple, 2006). However, it was not until the late 1950s when more recent scientific technological advances were made that the wonder of radioactivity began to be understood. Majority of the naturally occurring isotopes had been

acknowledged and their abundance determined, instrumentation with the correct and necessary sensitivity had been developed, isotopic tracers are also available in the prerequisite quantities and purity, and the half-lives of the long-lived radioactive isotopes were reasonably well known. By the beginning 1960s, most of the major radiometric dating techniques currently in use had been tested and their broad limitations known (Dalrymple, 2006).

It is scientifically well known that there is no technique that is ever completely perfected, and therefore refinements continue up to date, however for more than two decades radiometric dating techniques have been applied to define consistently the ages of the Earth, Moon, rocks and meteorites (Dalrymple, 2006). Radiometric dating is mainly centered on the decay of long-lived radioactive isotopes that occur naturally in rocks and minerals. The parent isotopes decay to stable daughter isotopes at rates that are able to be measured experimentally and being effectively constant over time irrespective of physical or chemical circumstances. Numerous long-lived radioactive isotopes are applicable in radiometric dating in various ways or techniques to determine the ages of minerals, rocks and organic materials.

Decay schemes are used separately in most cases to determine ages (e.g., Rb-Sr) and in combinations (e.g., U-Th-Pb). Each of this decay series has exclusive characteristics that make it applicable to a particular dating techniques for geologic situations. For instance a method focused on a parent isotope with a very long half-life, such as samarium ( $^{147}\text{Sm}$ ) of half-life  $1.06 \times 10^{11}$  years, is not useful for determining the age of a rock only a few million years old because of the insufficient amounts of the daughter isotope accumulated in this short period of time (Dalrymple, 2006). Similarly, the  $^{14}\text{C}$  dating method is very crucial in obtaining ages of certain types of fresh organic material and is impracticable on ancient granites. Dating techniques can work only on closed systems or only on open systems. This means that not all methods are applicable to all limestones of all ages. A key role of a dating specialist (Geochronologist) is being able to apply correct technique for the particular problem that need to be unraveled, and to design the investigation in such a way that there will be checks on the consistency and correctness of the results (Dalrymple, 2006) .

Internal checks for a number of methods is done to provide exactness of the data or lack of evidence for reliability. Relation order of rock units as perceived in the field is normally used as evidence to verify radiometric ages, in most cases for ages based on other decay schemes, or ages on several samples from the same rock. The ages of rock formations are rarely based on a solitary, isolated age determination measurement. On the other hand radiometric ages

correctness assurance is possible and practical, and its done by considering other relevant data (Dalrymple, 2006).

**Table 1:** Principal parent and daughter isotopes used in radiometric dating

Parent isotope	End product (daughter) or stable isotope	Half-life (years)
Potassium-40 ( $^{40}\text{K}$ )	Argon-40 ( $^{40}\text{Ar}$ )	1.25E+09
Rubidium-87 ( $^{87}\text{Rb}$ )	Strontium-87 ( $^{87}\text{Sr}$ )	4.88E+10
Carbon-14 ( $^{14}\text{C}$ )	Nitrogen-14 ( $^{14}\text{N}$ )	5.73E+03
Uranium-235 ( $^{235}\text{U}$ )	Lead-207 ( $^{207}\text{Pb}$ )	7.04E+08
Uranium-238 ( $^{238}\text{U}$ )	Lead-206 ( $^{206}\text{Pb}$ )	4.47E+09
Thorium-232 ( $^{232}\text{Th}$ )	Lead-208 ( $^{208}\text{Pb}$ )	1.40E+10
Lutetium-176 ( $^{176}\text{Lu}$ )	Hafnium-176 ( $^{176}\text{Hf}$ )	3.5E+10
Rhenium-187 ( $^{187}\text{Re}$ )	Osmium-187 ( $^{187}\text{Os}$ )	4.3E+10
Samarium-147 ( $^{147}\text{Sm}$ )	Neodymium-143 ( $^{143}\text{Nd}$ )	1.06 E+11

## 1.2 Problem Statement

Thermo-Luminescence dating is a technique that requires the measurement of the rate of delivery of radiation dose from the sample and its environment (Prescott and Hutton, 1995). However the dose rate might not be constant during accumulation in the sample. Thermo-luminescence from limestone has been employed to determine the time since the calcite material has been exposed to sunlight (Galloway, 2003). (Døssing et al., 2009), used Pb isotopic ratios obtained from individual Banded Ironstone Formations (*BIFs*) mesobands and associated volcanic and sedimentary rocks to calculate the depositional ages of the Neoproterozoic

Tati Greenstone Belt (NTGB), north-eastern Botswana and it was deduced to ages of around  $1976 \pm 88$  MY.

It is also prominent that there is little information in the literature on optical stimulation of luminescence studies from  $\text{CaCO}_3$  samples in Gaborone. Dating for the settlement of first human being in Botswana and the world as a whole, and the time of when some certain events happened is always a challenge. Thus dating of limestone using any paleodosimetric methods such as thermoluminescence (TL) has challenges (Guibert et al., 1998) due to the presence of heterogeneities in the radiation field caused by variations in the radiochemical composition within the irradiating limestone in Gaborone.

On completion of the study, this will enable the community of this area and the country of Botswana as a whole to understand how long the limestone of Gaborone has existed since their last formation (or disequilibrium), and also when human and natural events occurred, since limestone is one of the major components for human shelter construction.

In this research thermoluminescence dosimetric characteristics of the natural calcite (limestone) from Gaborone were studied to investigate their ages in comparison with those obtained by ICP-MS isotopic ratio technique. Based on available research there is no published research on Thermo-Luminescence and isotopic ratio dating of limestone using uranium series measured by electronic personal dosimeter (EPD) in Gaborone. Hence there is a scientific gap that needs to be investigated. In relation to this area of study there are, therefore calls for more studies to be conducted. Thus, we found it imperative and interesting to undertake this study on the Thermo-Luminescence and isotopic ratio dating of limestone samples from this area using uranium series measured by electronic personal dosimeter, gamma spectrometry and ICP-MS isotopic dating.

It is envisaged that this research will shed light on the geological events that affected or caused the alterations to the underground geochemistry of Gaborone and also provide a baseline information to other scholars in the future who will conduct a similar research.

### **1.3 Research Aim and Objectives**

#### **1.3.1 Aim**

The aim of this research was to investigate the application of Electronic Personal Dosimeter in Thermo-Luminescence and Isotopic Ratio Dating of limestone using uranium Series

#### **1.3.2 Specific Objectives**

In order to investigate the aim of this study, it was achieved via the following specific objectives:

- a) Evaluating the limestone sediments deposits in Gaborone at different topographic locations as affected by natural and human activities
- b) Determining the ages of the limestone samples using Thermo-Luminescence (TL) dating via uranium series data measured by electronic personal dosimeter (EPD)
- c) Determining the ages of the limestone samples using ICP-MS Isotopic Ratio Method for dating of the (U -Pb) radionuclides in the samples
- d) Compare TL dating and Isotopic Ratio (IsR) dating results with Concordia plots using the Isoplot Code.
- e) Provide a possible recommendation for an integrated (TL – IsR) dating technique

## CHAPTER 2: LITERATURE REVIEW

### 2.1 Background

Dates of natural and man-made happenings are a very important aspect of human livelihood awareness and understanding of evolution, as it is noticeable that priests, astronomers, philosophers and other educated people of the world, and other societies, already wanted to know more about creation and past times. In this context, one of the important questions has been to establish the origin and age of the Earth and Cosmos. However, these problems remained unsolved or were answered by rough estimates only, until radioactivity was discovered in 1896 and enabled an accurate dating (Von Gunten, 1995b).

It is noted that until the 18<sup>th</sup> century, the Bible which is assumed to be the oldest book, set the age of the Earth very accurately to 4004 years. Up to date creationists derive from studies of the Old Testament an age between 6000 and 10,000 years. It was at the end of the 19<sup>th</sup> century that Lord Kelvin used heat balances to estimate the Earth's age to be from 50 to 100 million years (Von Gunten, 1995b). By then already geologists concluded from many observations that this age was too short. And subsequently the discovery of radioactivity by Becquerel in 1896 (Von Gunten, 1995b) and the demonstration of heat evolution in this process by Curie and Labored, Lord Rutherford recognized in 1904, that Kelvin's Earth's age was indeed much too short, because he had neglected the important additional heat source in the interior of the Earth.

For the first time using a decay constant, Rutherford estimated the Earth's age from the amount of helium in uranium minerals, to 500 MY (Von Gunten, 1995b). Assuming, without experimental verification, that lead was the final product in the decay chain of uranium, Boltwood assigned 1907 MY about the same age value to uranite samples. Based on the first modern geological time scale, Holmes attributed, in 1913, an age of 1600 MY to certain archaic rocks (Von Gunten, 1995b).



The study of the Aeolian sand unit that covers the Middle Stone Age deposits at Blombos Cave on the southern Cape coast, turned out the belief that Aeolian sand deposits contained some culturally important artefacts, such as bone tools, engraved ochre pieces, and numerous worked lithics (Jacobs, 2003). Optical dating was used to date the Aeolian sand and two other remnants of the sand dune formed against the coastal cliff. The single-aliquot regenerative-dose (SAR) protocol was used to determine the dose received since deposition wherein measurements were made on 5 mg aliquots of purified quartz grains. Several internal check procedure results were

reported and at least 15 replicate dose determinations were presented for each sample. By combining these dose values with the measurements of the radioactive content of each sample, it resulted in an age of  $69.2 \pm 9$  ka for the part within the cave, and a mean age of  $70.1 \pm 1.9$  ka for all three dune samples and this provided a minimum age for the Middle Stone Age material at Blombos Cave (Jacobs, 2003).

Optical dating provides a straight forward means of dating sedimentary units, with the age of last exposure to sunlight being obtained from measurements of the optically stimulated luminescence (OSL) and the radioactive content (Jacobs, 2003), and it is apparent that optical dating is right for providing chronological information for sediments regarding the Middle Stone Age in Southern Africa. Some studies of the OSL behavior of quartz from Australian sand dunes, lately have steered to the development of an improved laboratory process for measuring the radiation dose to which materials have been exposed in their environment, this dose is called the equivalent dose ( $D_E$ ). The decay of elements in the Uranium and Thorium decay chains, and the decay of  $^{40}\text{K}$ , with an insignificant influence from cosmic rays, yield radiation in the environment (Duller and Wintle, 2012). In nature, minerals of quartz, feldspar, mica, calcite (limestone), etc. are continuously irradiated by  $\alpha$ ,  $\beta$  and  $\gamma$ -radiation resulting from the decay of members of the natural Uranium and Thorium decay chains, or the decay of  $^{40}\text{K}$  (Mercier, 2007). Whereby, atoms are ionized and the electrons are trapped in crystal defects, from where they cannot escape without an external excitation.

## 2.2 Thermoluminescent Dating

Luminescence dating is premised on the fact that several commonly occurring minerals (e.g. quartz and many feldspars) can be used as natural dosimeters, recording the amount of radiation to which they have been exposed (Duller, 1995). A known radiation dose to which the sample has been exposed since some event (such as the deposition of the sediment), and the radiation dose to which it is exposed per year as a result of the radioactive decay of Potassium ( $^{40}\text{K}$ ) and the Uranium and Thorium decay chains present in the surrounding materials can be used to calculate the age of the sample using the simple equation

$$\text{Age} = \frac{\text{ERD}}{\text{DR}} \quad (1)$$

Where;

ERD is the Equivalent Radiation Dose (Gy), DR defines the Dose Rate (Gy/ka),

Equivalent radiation dose of the sample can be determined by luminescence measurements. In the past 25 years considerable work has been done to determine optimal ways of measuring this quantity (Duller, 1995).

In the application of luminescence to the dating of geological or archaeological materials, equivalent dose is used to estimate the extent to which the sample has been exposed to ionizing radiation since the event that is to be dated. This quantity is presented as the equivalent dose ( $D_E$ ) or paleodose ( $P$ ). The single aliquot technique used to measure  $D_E$  can be categorized into three types;

- Additive dose,
- Regeneration, and
- Single aliquot regeneration on additive doses (SARA).

Two types, Additive dose and Regeneration are based on similar techniques used in conventional several aliquot luminescence dating and SARA is a composite technique combining the additive dose and regeneration elements procedures (Duller, 1995).

Limestone materials show TL, whereas aragonite shells do not (Johnson, 1960), and that materials that belong to a given taxonomic grouping have a tendency to have similar and analytical TL properties. TL on some species of limestone material remains in Pectinidae and Ostreidae family show TL physiognomies comparable to those of the albicans. The upper measurable limit by TL dating for such fossil limestone materials was about  $6 \times 10^5$  years. Many fossil corals have been found in limestone having transformed to calcite, but few fossil corals have remained as aragonite, which can be dated by the use of uranium- series dating methods (Ninagawa, 2001).

Dating of limestones by Thermo-Luminescence (TL) is of major interest in archaeological and quaternary research, since calcium carbonate is found in a large number of materials, a lot of different events could be dated, for instance the last heating of a fire stone, the growth of shells and the crystallization of calcite in carbonate deposits (Roque, 2001). A new archaeological potential of calcite has also been explored quite recently, mainly dating the burial of megaliths and architectural elements made of marble or limestone, by studying the sensitivity to light of some defects in calcite crystals. Indeed, TL dating of carbonate material broadens the horizons

of the methodological possibilities and permits multichronological approaches (TL,  $^{14}\text{C}$ , ESR, U - Th), for the same event that are to be dated (Roque, 2001).

Absolute age determinations of calcite formations in caves such as Stalagmites are often of archaeological interest, especially if relics of prehistoric life are chronologically interrelated to such "speleothems". Because the growth rate of stalagmites should be low or even zero during the ice ages, paleoclimatical information may also be obtained from the frequency distribution of speleothems ages determined so far. To satisfy oneself about the reliability of uranium series age dating, it is necessary to apply other absolute dating techniques. A comparison of  $^{230}\text{Th}$  /  $^{234}\text{U}$  ages and  $^{14}\text{C}$  data revealed, that a subsequent contamination of speleothems up to a few per cent of present  $^{14}\text{C}$  activity is, apparently quite frequent (Bangert, 1980).

Since prehistoric men frequently used limestone caves as their domicile or shelter, today many remains of their lives are covered by subsequently precipitated calcite formations. Such "speleothems" are usually regarded to be a most suitable material for dating purposes, and they are not altered as is bone material after long periods of storage. Uranium series dating seems to be a most reliable and rather frequently used technique to determine the formation age of such speleothems. A few other methods have been applied, but of these only  $^{14}\text{C}$ , Thermo-Luminescence and electron spin resonance (ESR) proved to be quite successful as well. From the three daughter nuclides of the uranium decay chain with known longevity, the isotope  $^{230}\text{Th}$  is commonly believed to be the most useful one for dating via radioactive disequilibria (Bangert, 1980).

Dating by means of luminescence involves destruction of the minerals crystal lattice and the structural faults by ionizing radiation. The destructive process energy comes from the surrounding radioactive nuclides sediment, secondary cosmic rays and the sample itself. Thus this absorbed dose (paleodose) is continual bagged in the crystal and the electrons move to an excitation state. In the process electrons in their excited metastable state reside over a long period of time enough to permit a dating technique application (Richter, 2007). The dose rate, defined as the ionizing radiation per unit time, is directly proportional to the paleodose of the sediment position of the sample. Dose rate lends dating applications the capability to time: such capability as used in uranium series dating of limestones becomes a possibility. Electrons are caused to ease to a ground state and a photon is released (luminescence process) when they are exposed to light or heat. High enough temperatures in the region of  $400^{\circ}\text{C}$  drain all electrons

relevant to the luminescence method used; then the clock is set to zero. The strength of the luminescence indicator (number of photons emitted) is directly proportional to the total absorbed dose in a crystal and is therefore a function of exposure time to radiation (Richter, 2007).

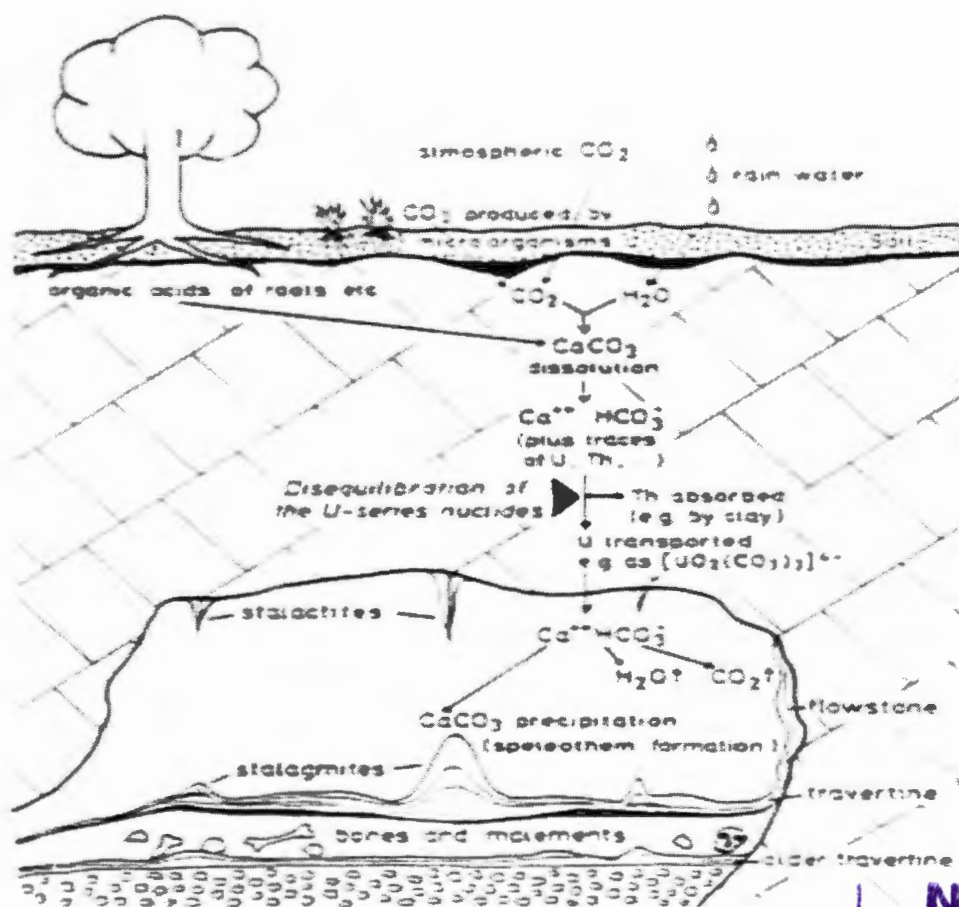
The accumulation of the dose or photons in the limestones begins with formation of the mineral. This notwithstanding, in most dating applications related to earth, curiosity lies in the time that would have passed since human activity took place, such as fire or other related events of human settlement, for an example sedimentation of housing remains in case of Optically Stimulated Luminescence (OSL) dating. The limestone therefore should have either exposed to light or heated at the time of interest in the distant past. Subsequently protection of deposition from light is essential. This depositions are the radiation dose and thus a latent luminescence signal is stored until the time it is taken to the laboratory for measurement (Richter, 2007). Thus the formula for age calculation is:

$$\text{Age} = \frac{\text{Paleodose}}{\text{Dose rate}} = \frac{P_{(\text{Gy})}}{\dot{D}_{(\text{Gy.a}^{-1})}} \quad (2),$$

Where; P is the paleodose, P, in Gy and,  $\dot{D}$ , is the dose rate in Gy per time unit (ka).

The paleodose is a term synonymous to absorbed dose in TL dating. This absorbed dose is attained from the TL signal, which is measured by heating limestone aliquots at a constant temperature rate, paleodose can be measured from the TL signal as a result of the production the glow curves (Richter, 2007).

Figure 1 below shows the basis of U-series dating via the activity ratio of  $^{230}\text{Th} / ^{234}\text{U}$ . The trace element uranium is easily dissolved and transported by karstic, carbonate-rich waters seeping through the limestone rock. Thorium, however, is tightly adsorbed by clay minerals always present in the hair-cracks and crevices of the roof limestone (Bangert, 1980).



**NWU  
LIBRARY**

**Figure 1:** The root of U-series dating via the activity ratio of  $^{230}\text{Th} / ^{234}\text{U}$  (Bangert, 1980)

It is for this reason that, in the members of the  $^{238}\text{U}$  series (Figure: 2) the thorium isotope  $^{230}\text{Th}$  is practically absent in the speleothems- forming dripping waters of the cave, whereas  $^{238}\text{U}$  and  $^{234}\text{U}$  are present and get into the growing calcite formations. Therefore, the activity ratio of  $^{230}\text{Th} / ^{234}\text{U}$  is practically zero in very young stalagmites or other recently precipitated speleothems up to approximately  $10^3$  years of age. The  $\alpha$ -decay of  $^{234}\text{U}$  now slowly generates  $^{230}\text{Th}$   $\alpha$ -activity again, so that the  $\alpha$ -activity ratio of  $^{230}\text{Th} / ^{234}\text{U}$  will constantly increase for about  $4 \times 10^5$  years (Stanley, 2012).

The U-Th-Pb decay chains are deemed to be the most accurate possibilities for measurements of geological samples with ages greater than 30 million years. The stable end products in the decay chains of  $^{238}\text{U}$  ( $T_{1/2} = 4.468 \times 10^9$  years),  $^{235}\text{U}$  ( $T_{1/2} = 7.038 \times 10^8$  years), and  $^{232}\text{Th}$  ( $T_{1/2} = 1.405 \times 10^{10}$  years) are the lead isotopes  $^{206}\text{Pb}$ ,  $^{207}\text{Pb}$  and  $^{208}\text{Pb}$ , respectively (Yip, 2008). The abundance of these lead isotopes in a sample might be used to determine the time since the formation of the sample as a closed system. In modern methods, the lead isotopes are always determined by thermal ionisation mass spectrometry, and the amount of the non-radiogenic

$^{204}\text{Pb}$  can be used to estimate and correct the concentrations of the other lead isotopes that were in the sample at time  $t = 0$ , (Von Gunten, 1995b).

The age based on the decay of  $^{238}\text{U}$  is obtained by use of Equation (3a & 3b) below:

$$t = \frac{1}{\lambda_{238}} \ln \left\{ 1 + \left[ \frac{{}^{206}\text{Pb}_t - {}^{206}\text{Pb}_0}{{}^{238}\text{U}_t} \right] \right\} \quad (3a)$$

And to calculate  $^{206}\text{Pb}_0$  use

$${}^{206}\text{Pb}_0 = 5 * {}^{204}\text{Pb} \quad (3b)$$

These equations are also applicable for  $^{235}\text{U}/^{207}\text{Pb}$  and  $^{232}\text{Th}/^{208}\text{Pb}$ . Contrasting of different dating methods can be used for the validation of the closed system condition, in this study the use of isotopic ratio dating is carried out to verify the results for EPD dating using uranium series as a way of validating that the results obtained using EPD dating methods are true and thus can be trusted.



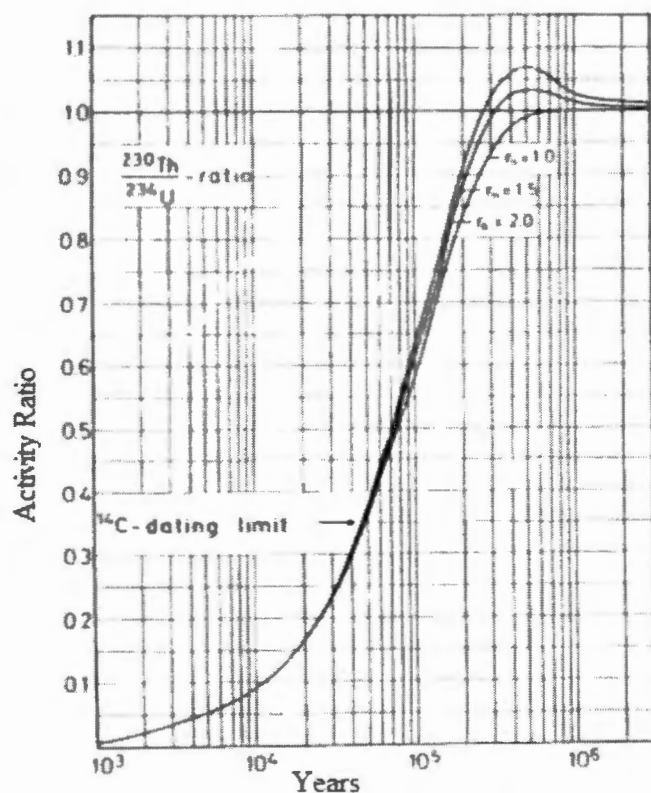


**Figure 3a:** The time dependent change of activity ratios of  $^{230}\text{Th} / ^{234}\text{U}$  starting from different initial  $^{234}\text{U} / ^{238}\text{U}$  ratios ( $r_0$ ) (Bangert, 1980)

Each single growth zone is then dissolved in hydrochloric acid or nitric acid (HCl or  $\text{HNO}_3$ ), and the trace amounts of uranium and thorium are separately isolated by means of a specially developed chemical procedure as shown on Figure: 4. Artificially produced isotopes  $^{232}\text{U}$  and  $^{228}\text{Th}$  are added as tracers for the different uranium and thorium yields. After electroplating uranium on one polished stainless steel cathode and thorium on another, the  $\alpha$ -activities of the U- and Th-isotopes can be easily determined because of their very different  $\alpha$ -energies. This is usually done by means of a high-resolution silicon surface barrier detector, and the impulses are registered in a multichannel-analyzer according to their peak heights (Stanley, 2012).

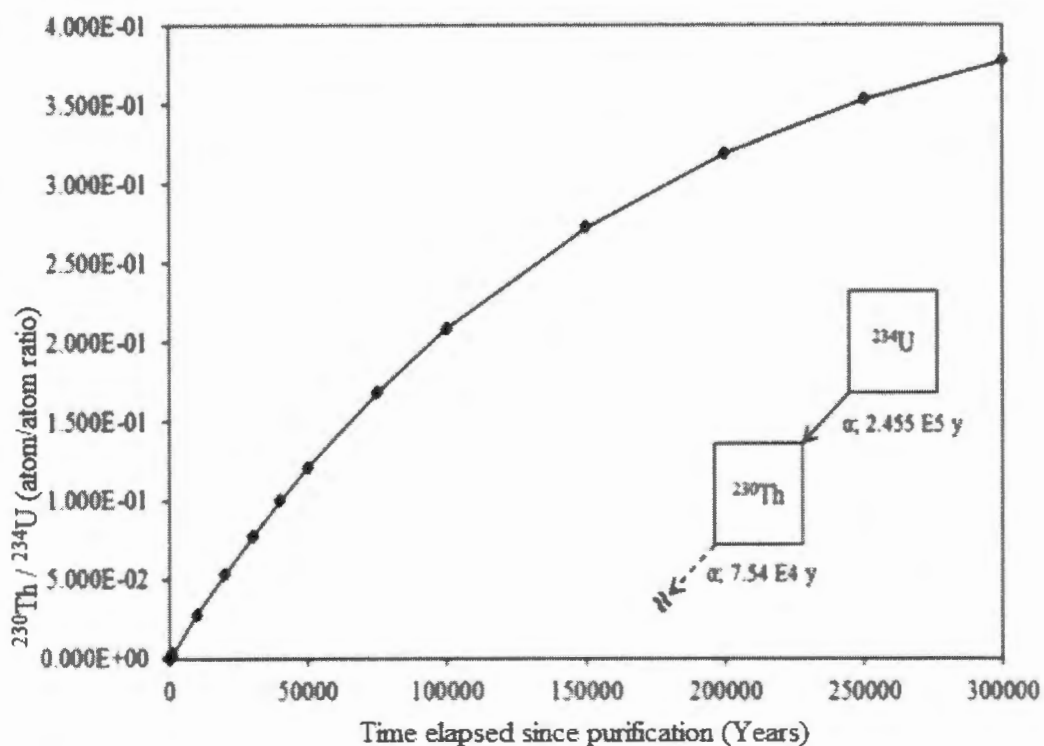
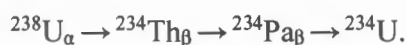


**Figure 3b:** A plot of the relationship between  $^{234}\text{U} / ^{238}\text{U}$  and age of a sample (Stanley, 2012)

There is a possibility that these conceptions and equations, if necessary precautions and factors are put into considerations can theoretically be used in all the uranium daughter nuclide relationships for the appropriate exchange of variables. It is worth noting that in most practices, the application of uranium chronometric associations variability is contributed by aspects such as; vast interferences, short lifespans or half-lives leading to partial windows of analytical opportunity, and lengthy lifespans or half-lives orchestrating to ultra-trace progeny ingrowth (Stanley, 2012).

Uranium-238 (238.050788247 amu) is a very common and abundant uranium isotope occurring natural, with an abundance of 99.2745% and belonging to the  $4n+2$  parent uranium decay series,  $^{238}\text{U}$  is a long-lived radionuclide ( $T_{1/2} = 4.47 \times 10^9$  years) which decays to short-lived  $^{234}\text{Th}$  ( $T_{1/2} = 24.10$  days) by discharge of  $\alpha$ -particle (4198.3 KeV). The correlation of  $^{238}\text{U}$  and  $^{234}\text{Th}$  as a function of time is shown in Figure 3b above as time elapsed since material purification, this is achieved by an assumption of that complete removal of thorium took place at  $T_0$  (Stanley, 2012). This is attained as the system approaches secular equilibrium as a result of the high constant activity of  $^{234}\text{Th}$  leading to an observation of  $^{234}\text{Th}/^{238}\text{U}$  isotopic ratio minimal change after a period of 150 days following purification, and thus a limited window

period for age-dating methodology as a result of the chronometric value and limits of less than 5 to 6 months old standardization. Due to this window limitation, chronometric relationships are mired by the natural occurrence of  $^{238}\text{U}$  and becomes prone to producing subjective results for age-dating. Because of the limitations and interferences in the  $^{234}\text{Th}/^{238}\text{U}$  chronometer, makes it to be of insignificant use in safeguards investigations and nuclear forensics (Stanley, 2012). It is worth perceiving that the decay of  $^{238}\text{U}$  produces  $^{234}\text{U}$  as shown below:



The  $^{234}\text{U}/^{238}\text{U}$  ratio is not of critical chronometric significance because the progeny nuclides are recollected in the course of radiochemical purification, but it is of usage in relations to materials characterization (e.g. determining enrichment) as  $^{234}\text{U}$  abundance increases equivalently quicker than  $^{235}\text{U}$  in the process of enrichment. Thus the  $^{234}\text{U}/^{238}\text{U}$  ratio relationship full value still remains a belligerent point with regard to their high naturally variations (Stanley, 2012).

Uranium-236 (236.045568006 amu) is an artifact of  $^{235}\text{U}$  (n,  $\gamma$ ) reactions taking place in reactor settings, naturally and by decay of  $^{240}\text{Pu}$ . Although in most cases it has not been accounted for, it has recently surfaced that  $^{236}\text{U}$  is existent naturally at profusions of  $10^{-10}\%$  by the use of accelerator mass spectrometry (AMS) analysis. Uranium-236 is a member of the 4n Thorium decay series and it is a long-lived radionuclide ( $T_{1/2} = 2.342 * 10^7$  years) decaying to  $^{232}\text{Th}$ , a long-lived nuclide ( $T_{1/2} = 1.4 * 10^{10}$  years), by release of  $\alpha$ -particle (4494.3 KeV). The  $^{236}\text{U}$  and  $^{232}\text{Th}$  chronometric relationship provides a theoretically large window for analytical opportunity in age-dating techniques, based on assuming that thorium was completely removed at  $T_0$ , with a hypothetical material showing that  $^{232}\text{Th}/^{236}\text{U}$  ratio increases directly proportional in a high linearity style ( $R^2 = 0.9995$ ) for millions of years after the purification process (Stanley, 2012).

Nonetheless, the  $^{232}\text{Th}/^{236}\text{U}$  ratio is also of no chronometric importance in light of these contemplations and there is  $^{232}\text{Th}$  radionuclide which is naturally ever-present and thus a concern as it is able to interfere age dating accuracy. The results of this isotopic ratios would be susceptible to seem older than fitting and the parent nuclide in the chronometer being long-lived, and thus leading to a slight ingrowth of the progeny nuclides after purification and the modern analytical instrumentation limits are being probed as a result of this discoveries

(Stanley, 2012). Subsequently as the  $^{232}\text{Th}/^{236}\text{U}$  ratio is of no value to chronometry, the detection of  $^{236}\text{U}$  is of great importance to safeguards investigations and nuclear forensics. Uranium-236 is usually formed through the process of neutron capture and thus  $^{236}\text{U}/^{238}\text{U}$  ratios greater than  $10^{-9}$  may be used as a critical indicator to show the samples presence in the neutron flux or plutonium materials, and this makes  $^{236}\text{U}$  a key signature in determining the past processing and potential activities associated with a material involved (Stanley, 2012).

Uranium-235 (235.043929918 amu) is the second most and researched isotope of uranium occurring natural and having an abundance of 0.72%. It is a very crucial fissile radionuclide of interest in the uranium production based nuclear power plants and weapon fuels of various enrichment. It is part of the parent of the  $4n+3$  actinium decay series, also long-lived radionuclide ( $T_{1/2} = 7.04 \times 10^8$  years) and decays to shorter lived  $^{231}\text{Th}$  ( $T_{1/2} = 25.52$  hours) by the emission of an  $\alpha$ -particle (4397.8 KeV) (Stanley, 2012).

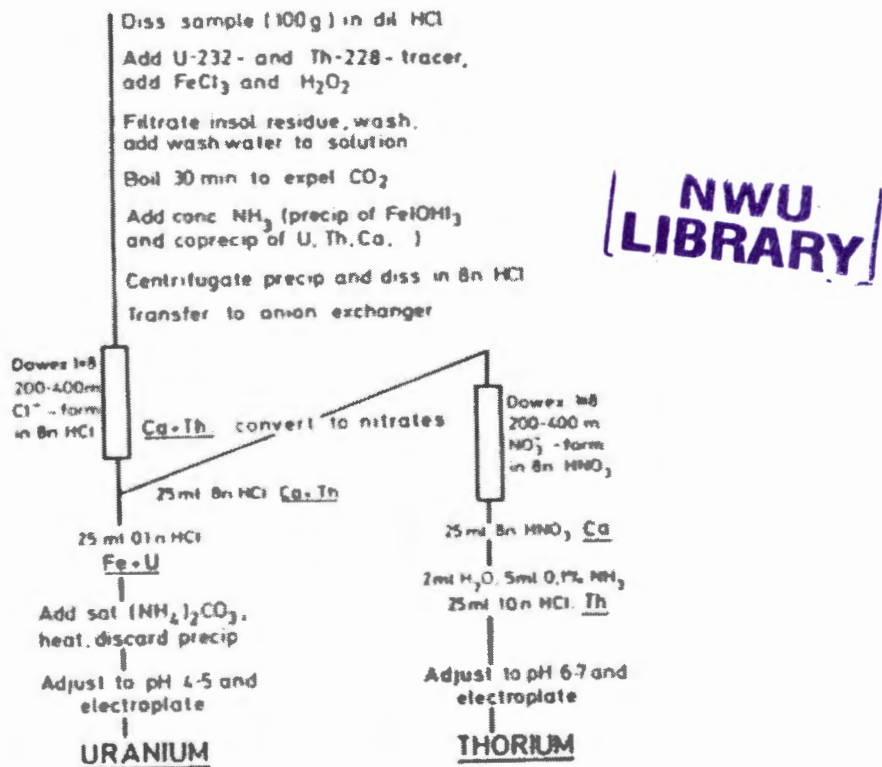
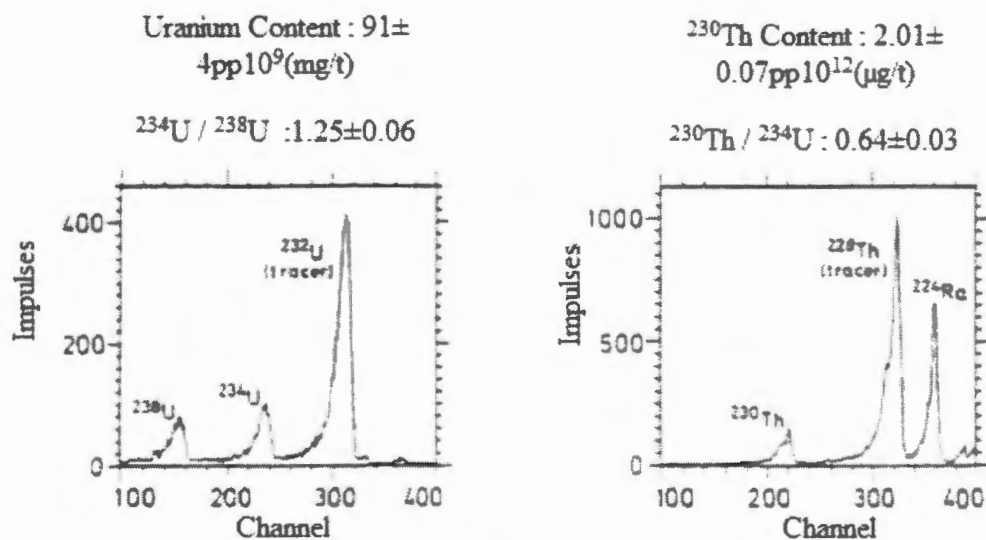


Figure 4: Chemical separation procedure for uranium and thorium (Duval, 2016)

In Figure 5 a pair of  $\alpha$ -spectra is presented giving the data needed for the  $^{230}\text{Th} / ^{234}\text{U}$  age calculation. Both the U- and Th-  $\alpha$ -spectrum are from an inner section of a stalagmite found in a small cave near Letmathe in the Sauerland area in Germany, the  $^{230}\text{Th} / ^{234}\text{U}$  activity ratio of 0.64 corresponds to an age of  $1.1 \times 10^5$  years, the average formation age of the whole growth layer (Bangert, 1980).



**Figure 5:** Alpha spectra of uranium and thorium isotopes (Bangert, 1980)

Many electrically non-conducting minerals, which were exposed to artificial or natural irradiation, emit light when they are heated. This thermo-luminescence phenomenon was observed in 1663 by Boyle, when he heated diamond. The age of a sample was deduced from the effects of the radiation energy that was deposited and has accumulated in the sample since its formation (Mercier, 2007).

Due to the long half-lives of the main radionuclides involved, the radiation dose rate can be assumed as constant. In the Thermo-Luminescence method the external excitation is promoted by heating. Part of the trapped electrons combine with holes, others form luminous centers. With increasing temperature, one may observe several light signals. First, the least stable trapped electrons are released, and at higher temperature, the most stable ones. Thus, a Thermo-Luminescence curve is obtained which is characteristic for a sample and its irradiation history (Von Gunten, 1995b).

If a sample is heated for a second time, no further light signals are observed. However, if such annealed crystals are exposed to a radiation source, a new Thermo-Luminescence curve is

obtained which differs from the first one by showing peaks at lower temperatures (i.e. above 100°C), in addition to the signals at higher temperature (230 – 400°C) which were already observed during the first heating. For applications, it is advisable to use the signals emitted at high temperature. Artificial irradiation experiments with increasing radiation doses have shown that the high temperature Thermo-Luminescence is proportional to the irradiation dose of the material (Von Gunten, 1995b). If the investigated sample remained in the same environment during its whole history, then the irradiation dose rate can be assumed to be constant, and it is in principle possible to evaluate the age of the sample from the magnitude of the high temperature Thermo-Luminescence peak (Von Gunten, 1995b).

The age of a sample can be calculated from the following relation, if the annual irradiation dose is exactly known:

$$\text{Age} = \frac{\text{Natural Dose}}{\text{Annual Dose}} \quad (4)$$

The natural dose is the total radioactive decay energy acquired per unit mass since the formation (e.g., crystallization) of a sample. The annual dose is the energy corresponding to the radioactive decay of the nuclides in the sample. This emitted decay energy is not related in a simple way to the energy acquired by the sample. By far the largest amount of energy is contributed by  $\alpha$ -decay of the Uranium and Thorium decay families. But the range of  $\alpha$  - particles in solid matter is only 20 to 50  $\mu\text{m}$ , depending on their energy and the density of the material. On the other hand, the ranges of  $\beta$ -particles in solids are of the order of millimeters, and  $\gamma$ -rays travel much farther and have only a few interactions when traversing the solid material. It is, therefore, necessary to establish efficiencies for the energy deposition for each type of radiation and material. Furthermore, corrections for a lack of homogeneities in the samples have to be made (Von Gunten, 1995b).

The range of linearity between the dose and the Thermo-Luminescence signal is limited: at higher doses a saturation effect is observed. For quartz, saturation occurs at 100 to 500 Gy (10 to 50 krad), whereas calcite can accept 3000 Gy (300 krad). Despite these problems, Thermo-Luminescence has been successfully used to date archaeological (e.g. ceramic artefacts, burned stones used as Kitchen utensils, stone tools. etc.), and geological samples (e.g., recent volcanic rock, young calcite formations in caves, very fine aeolian deposit in which the Thermo-Luminescence was annealed by exposure to bright sunlight when they resided on the surface, etc.) (Von Gunten, 1995b).

Thermo-Luminescence is undoubtedly related to the age of the samples. However, its application is not as straight forward as in many of the other dating methods, and practically each application has its specific and inherent problems. The method should not be applied blindly. But if all the problems are treated properly, it can be used to assess a time-range which falls between that of the applicability of  $^{14}\text{C}$  and the lower limit of the potassium-argon method (Von Gunten, 1995b).

### **2.3 Benefits and limitations of Thermo-Luminescence**

Dating limestones by dosimetric approaches depends on sites surrounding. Thus they are predisposed to mistakes as a result of gradually changing surrounding conditions. The influence of surrounding conditions on age dating result relies mostly on the proportion of the numerous factors to the totality of all factors. Having all this predicaments in mind, they have to be considered at all times and be evaluated for all the results. From known and applicable dosimetric means of dating, thermoluminescence on rock heated material is the least sensitive based on the stable internal dose rate of all the samples. Evidence shows little or no internal dose rates present for materials used in Optically Stimulated Luminescence (OSL) dating of sediment. Additional to the problems arising from the aforementioned variability, OSL dating potential problems are in the completeness of the zeroing of the signal and the possible incorporation of sediments of different ages (Richter, 2007).

It is noted that Infrared Stimulated Luminescence (IRSL) dating method on sediment has a small stable internal dose rate like that in flint, often times affected by an anomalous loss of signal though, and leading to a marked underestimation. Uncertainties of the uptake history of  $^{238}\text{U}$  into the limestone samples over time give problems that affect Electron Spin Resonance (ESR) dating, whereas U-series dating of limestones requires the assumption of the presence of a closed system. Radiocarbon ( $^{14}\text{C}$ ) dating, a frequently applied method, can be questioned quite frequently when it provides age for samples that are associated with past human activity (Richter, 2007).

Furthermore, in most cases the time scale provided is not linear, and therefore calibration of results must be done so that there can be verification of the correctness of the results, as an agreed method does exist to an extent up to 20 ka. A recurring criticism of TL dating relates to the huge uncertainties obtained, but the sum average of weighted uncertainties for TL dating results is akin to calibrated single  $^{14}\text{C}$  data. A series of measurements obtained by the TL

method cannot be averaged after the statistical process of calibration of the individual results, thus leading to exaggerated age estimate ranges for multiple dating (Richter, 2007).

The entire age of the parent material can be established by measuring the amount of radioactive decay of a radioactive isotope with a known half-life. Radioactive isotopes have been used in the past and are still being used today for this purpose, and depending on the decay rate, isotopes enable dating of different geological material ages. In addition, isotopes that decays slowly are more useful in dating longer periods of time, although its results are less accurate in absolute years, with an exception of radiocarbon dating method (McGoodwin, 2010).

Most of these techniques concentrate on the abundance measurements on the increase of radiogenic isotope, which is the decay-product of the radioactive parent isotope. To achieve correct and reliable results, it is recommended from previous studies that the use two or more radiometric dating methods on the same sample be a pre-requisite for acceptance of any dating results. It is of view that most of the radiometric dating methods suitability is on geological time frames only, whereas some such as radiocarbon dating method and  $^{40}\text{Ar}/^{39}\text{Ar}$  dating method can be extended into timing of early human life activities and the recorded history (McGoodwin, 2010).

From uranium to lead and lead to uranium ratio dating technique, the measurement of ratios of two lead isotopes ( $^{206}\text{Pb}$  and  $^{207}\text{Pb}$ ) which are products from the decay of  $^{235}\text{U}$  and  $^{238}\text{U}$  in a geological material, is a method often used to trace mineral zircon in igneous rocks, it is one of the two most commonly used, and hand in hand with argon-argon dating for geologic dating. Uranium to lead ratio dating is more applicable and suitable to samples older than 1 million years of age (McGoodwin, 2010).

## CHAPTER 3: METHODS AND MATERIALS

### 3.1 Geographical location of samples collection site

A total of 20 limestone samples were collected in Gaborone area of Mogoditshane-Tsolamosese (Block 4) at randomly selected ancient human settlement area  $\pm 100$  meters apart from each other and their geographical location coordinates noted as in Table 2 below.

**Table: 2.** GPS coordinates of the sample sites

Sample	Sample Coordinates	
	Latitude	Longitude
A	-24.65402	25.85594
B	-24.65340	25.85647
C	-24.65345	25.85688
D	-24.65348	25.85759
E	-24.65380	25.85787
F	-24.65423	25.85810
G	-24.65465	25.85799
H	-24.65468	25.85764
I	-24.65457	25.85710
J	-24.65452	25.85685
K	-24.65468	25.85655
L	-24.65469	25.85654
M	-24.65485	25.85650
N	-24.65498	25.85640
O	-24.65500	25.85626
P	-24.65500	25.85604
Q	-24.65517	25.85587
R	-24.65530	25.85576
S	-24.65534	25.85553
T	-24.65535	25.85526

The study area is shown in Figure 6 and Figure 6a below for the map of Gaborone where the samples were collected showing the coordinate points for each sample as a dot and labelled with each sample ID.

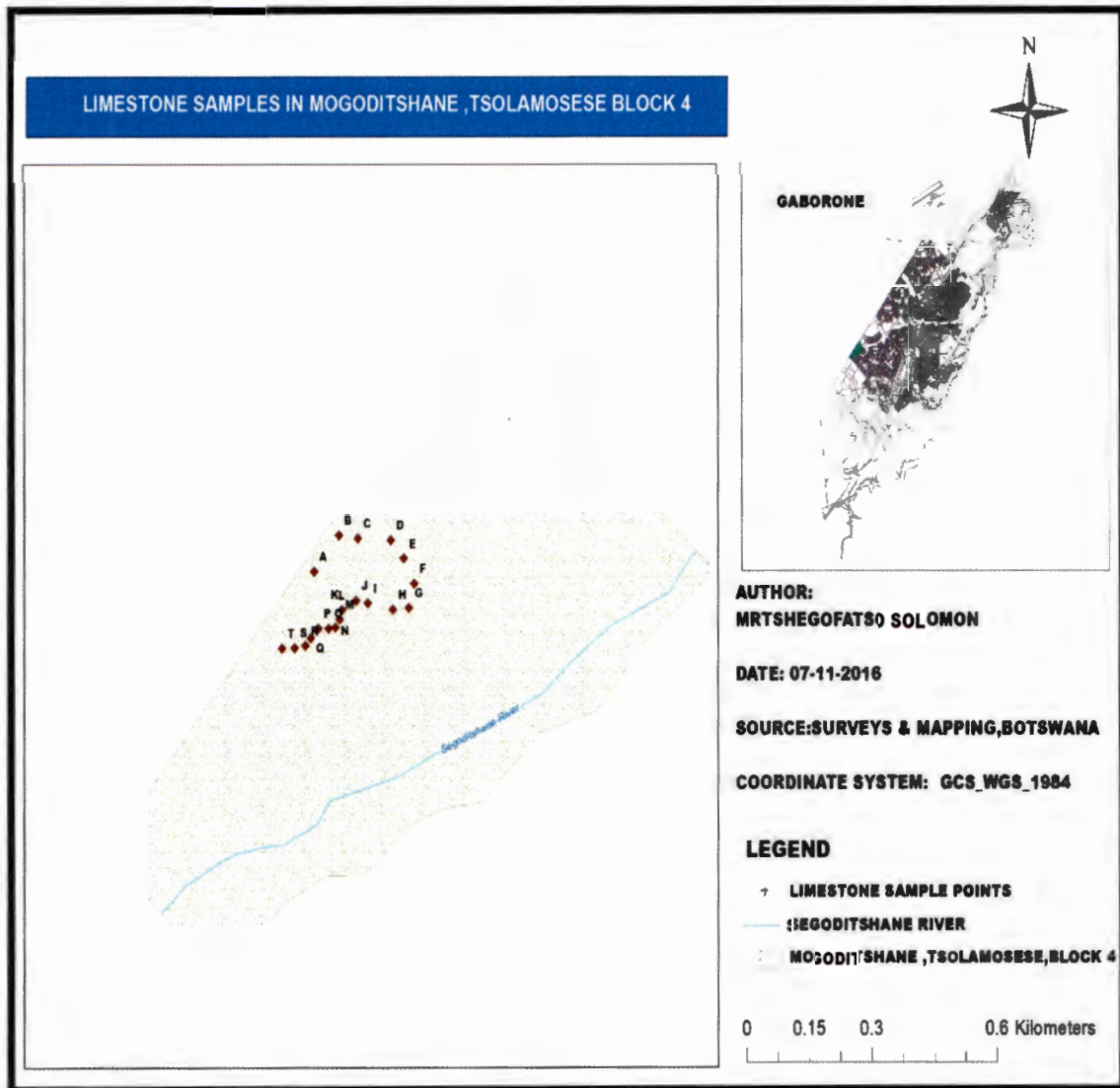


Figure 6: Map of Gaborone showing GPS locations of sample collection.





**Figure 6a:** GPS locations of sample collection.

### **3.2 Techniques of radioactive dating**

There are different types of techniques or methods used when it comes to radioactive dating by means of Thermo-Luminescence that have proved to be reliable in the past. The use of passive and active dosimeters to measure the radiation dose for radioactive dating yields acceptable results.

The method described by Stanford (2009), of (surface exposure dating with cosmogenic isotopes) describes the siliceous artifacts dating themselves. The limiting requirements for dating siliceous artifacts is that they should continuously have been exposed during fabrication and not having been previously exposed or unless the time prior to exposures is able to be determined. By fulfilling the limiting requirements for dating, there is restraint. Historic tools and unknown age materials exposed thousand to millions of years can be dated. The isotopes used are  $^{26}\text{Al}$ ,  $^{10}\text{Be}$  and  $^{21}\text{Ne}$ , as they are produced within a rock when it is bombarded by cosmic rays. The amount of exposure concentration obtained gives a direct measure of time for the cosmic rays bombardment of the rock at the surface or near the surface (Stanford, 2009).

### 3.3 TL Emission and Dose Response

There is a research by (Moffatt, 2012) on Thermo-Luminescence whereby the following methodology was used; use of two aliquots of 180 mm and 250 mm diameter for each sample, measurements of TL being conducted at  $-271.15^{\circ}\text{C s}^{-1}$  from  $0^{\circ}\text{C}$  to  $400^{\circ}\text{C}$ , and a reheat for background subtraction. The Risø TL-DA-8, with an EMI 9635QB 50 mm bi-alkali photomultiplier was used to undertake the runs (Moffatt, 2012). During TL emissions there was no filter used for detection of useful signals, and thus the spectral range was between 200 nm to 600 nm and peak response 400 nm approximately. Two runs were subjected to each aliquot. The first aliquot run of each sample measured the natural response of the samples and the second run of the first aliquot and all runs of the second aliquot measured the TL emission after an irradiation with beta at almost 10 Gy (Moffatt, 2012).

Due to the pyrex glass high sensitivity to radiation and having stable peaks, it was favored for survey of dose response. The main aim being to find out if during time-critical dosimetry accidents, whether glass could be used as a dosimeter. The UV band was also favored as its filters are definitely available and commonly used, thus tolerating prompt measurement in unadventurous dating laboratories. Eighteen pyrex aliquots of 180 mm -250 mm diameter grains were prepared and heated up to  $300^{\circ}\text{C}$  at  $-272.15^{\circ}\text{C s}^{-1}$  and the TL was measured using a 6 mm U340 filter which isolated the UV emission. Aliquots were then irradiated with a dose between 0 and 104 Gy. Mass normalization was done and aliquots irradiated again with a 27 Gy test dose and also reheated for checkup of any change in dose dependent sensitivity (Moffatt, 2012).

### 3.4 Thermo-Luminescence and Isotopic Ratio Dating

The methods that was used for this research was:

Thermo-Luminescence dating using electronic personal dosimeters (EPD) in combination with single aliquot regeneration on additive doses method (SARA) as described by (Duller, 2012) indicate that SARA procedure sensitivity change effects can be overcome by having three beta doses being irradiated in the laboratory instead of building up a full regeneration growth curve. This is done to compensate for the luminescence signals which embrace the natural signal, therefore allowing the regeneration  $D_E$  to be interpolated. This procedure is repeated on at least for three single aliquots of each sample and is repeated three times, having samples received a

radiation dose in addition to their natural radiation dose ( $D_n$ ) before the regeneration process (Duller, 2012).

Under Thermo-Luminescence dating, the use of both active and passive dosimeter was applied in combination to determine the actual and annual doses respectively. Electronic dosimeters give instant results when samples are being analyzed. The active dosimeter is sometimes referred to as an operational, alarm, or electronic dosimeter respectfully. As it provides instant display of the accumulated dose. They also have some extra functions such as alarm threshold settings for dose and dose rate values. This type of dosimeters have visual and audible indication of the dose rate levels. They require a battery to function and in most cases are used as complementary dosimetry in the areas of high radiation levels or for work and dose optimization purposes. While passive dosimeters store radiation energy in the form of light and thus require to be read using a TLD reader to retrieve the dose stored in the TLD chips.

#### **3.4.1 Method 1: Electronic Personal Dosimeter (EPD)**

Limestone samples ( $n = 20$ ) each weighing about 50g, were collected from the sampling site shown in Figure 6 and 7. Each sample was then crushed in a mortar and pestle into a fine powder. To ensure that the samples were not affected by light (dose zeroed by light), they were prepared and wrapped in a black plastic bag inside a dark room. The highest dose reading from each sample was determined using the electronic dosimeter (RadEye Thermo Fisher Scientific Messtechnik GmbH).

#### **3.4.2 Thermo-Luminescence Dosimeters (TLD)**

The 6600 TLD reader (Thermo-Fisher Scientific, Germany) was cooled down to a photomultiplier tube cooler noise temperature of  $9^\circ\text{C}$  using liquid nitrogen. The TLD 0011 cards were then annealed for about 13 seconds on average and at a temperature rate of  $25^\circ\text{C}/\text{sec}$  and  $300^\circ\text{C}$  maximum annealing temperature. Then aliquot of 1 g each were prepared from the powder samples for 2 replicates of each, which were then placed in the TLD 0011 cards positions iii and iv simultaneously . The 20 TLD 0011 cards were then read using the TLD 6600 reader and the WinRems software (Thermo Scientific, Radiation evaluation measurement system, version 8.2.3.0). The data from this software was exported to an Excel file for further processing.

### 3.5 Method 2: ICP – MS Isotopic Ratio

#### 3.5.1 Instrumentation

The Perkin Elmer, NexION 300Q, Inductively Coupled Plasma Mass Spectrometer (ICP-MS), (Perkin Elmer, United States of America) was used for all sample analysis in this work. It has a Quadrupole ion deflector that focuses the ion beam to the Dual mode detector. The Isotope-ratio precision of this instrument is defined for the isotope ratio of  $^{107}\text{Ag}/^{109}\text{Ag}$  internal standard using a 25  $\mu\text{g}/\text{L}$  solution, which is achieved by single-point peak hopping with a relative standard deviation ( $= 100 \times \text{SD}/\text{AVERAGE}$ , ((0)) of  $< 0.2\%$  RSD. The optimized operating parameters are summarized in Table 3.

**Table 3:** NexION 300q ICP-MS Instrumental Parameters (Bosnak, 2014)

Parameter	Value
Nebulizer	Glass concentric
Cones (Sampler, Skimmer, super-skimmer)	nickel
Spray Chamber	glass cyclonic
Sample Uptake Rate	300 $\mu\text{L}/\text{min}$
Plasma gas flow	18.0 L/min
Auxiliary gas flow	1.2 L/min
Nebulizer Gas Flow	0.98 L/min (Optimized for 2% CeO/Ce)
RF Power	1600W
Cell Gas	Argon
Detector Type	Dual mode
Sweeps/Reading	200
Readings/Replicate	10
Replicates per sample	2
Mode / Universal Cell Technology™	Isotope Ratio/Collision mode
Internal Standard	$^{107}\text{Ag}/^{109}\text{Ag}$ using a 25 $\mu\text{g}/\text{L}$ solution
Total integration time	3.4s

#### 3.5.2 Interference reduction

It is well established that if the elements do not have two non-radiogenic isotopes (e.g., Pb) or two more isotope ratio, then the internal standard normalization method cannot be used to make mass correction (Horn et al., 2000, Lin et al., 2016, Thirlwall and Anczkiewicz, 2004). Yet, we can use pseudo-internal standard normalization to determine the mass fractionation normalization for one element by directly applying this normalization to another element of similar or neighboring mass in the periodic table (Thirlwall and Anczkiewicz, 2004, Lin et al., 2016). In addition, it has been argued that UV radiation causes the photo-oxidation of  $\text{Tl}^+$  to  $\text{Tl}^{+3}$ , which then exhibits a different chemical behavior than its single ionic state in the presence of Pb, resulting in higher values of Pb/Tl and  $^{205}\text{Tl}/^{203}\text{Tl}$  ratios (Yip et al., 2008). On the other

hand, UV oxidation of Ag is known to significantly enhance  $\text{Ag}^+$  release (Mittelman, 2015), and thus samples can be handled even in the open laboratory

In the ICP-MS analysis of samples, the following molecular ions are potential sources of interferences; oxides, hydrides, hydroxides, nitrides (Horn et al., 2000, Thirlwall and Anczkiewicz, 2004, Verni, 2017). Their effect can however be reduced by using the Perkin Elmer NexION 300Q's desolvating nebulizer. Also, the instrument's quadrupole ion deflector focuses only the selected isotopes in the ion beam, to the dual mode detector. The other (interfering) ions are allowed to pass through to the waste (Mangum, 2015, Bosnak and Pruszkowski, 2014, Vilta, 2016). This capability of the NexION 300Q, combined with its Universal Cell Technology™, enables significant reduction in most or all the molecular ions in the sample (Lin et al., 2016).

### **3.5.3 Sample Run**

The samples were loaded on to the auto sampler and initialized using the ICP-MS Instrument Control (Data Acquisition) Software. The instrument was set to Isotopic Ratio Method, operated in the Collision Mode for mass energy discrimination and filtration against interferences (Vilta, 2016).

#### **3.5.4 ICP-MS Trace Calibration for trace element analysis**

Quality control samples such as blanks, duplicates, and certified reference material were included in the analyses (Keegan et al., 2008)

For analysis of trace elements, the Perkin Elmer, NexION 300Q, (ICP-MS), calibration uses a dual detector calibration solution as the atomic spectrometric standard, whose specifications are:

In the total quantitative method, the standards have 10 mg/L of Al, Ba, Ce, Co, Cu, In, Li, Mg, Mn, Ni, Pb, Tb, U and Zn. For every measurement, the instrument was set to run a blank and a standard check at every ten samples.

## **CHAPTER 4: RESULTS AND DISCUSSIONS**

### **4.1 Introduction**

The results are presented in three categories according to the technique used to collect the data, as follows:

- EPD /TLD (SARA) Technique data
- Gamma spectrometry data
- ICP-MS data
- U-Pb Concordia Plots

A total of 20 Limestone samples were collected in Gaborone area of Mogoditshane Tsolamosese Block 4 at randomly selected ancient human settlement areas  $\pm 100\text{m}$  apart from each other and their geographical location coordinates were noted.

## 4.2 EPD /TLD (SARA) Technique data

The results from the EPD/TLD (SARA) technique are shown in Tables 4 & 5 and Figure 8 & 9 below.

**Table 4:** TLD results for the sample aliquots, done on 27/11/2015

Sample ID	Position iii (Replicate 1)	Position iv (Replicate 2)	Average Doses ( $\pm 0.62699$ )	Units
PMT Noise	0.01469	0.01263		nC
Reference Light	87.62500	88.17400		nC
A	0.56503	1.69970	1.13236	mSv
B	0.17439	0.76287	0.46863	mSv
C	2.96373	0.50677	1.73525	mSv
D	0.34357	0.33219	0.33788	mSv
E	0.31071	0.07383	0.19227	mSv
F	0.54078	0.16936	0.35507	mSv
G	2.43555	0.94302	1.68929	mSv
H	1.13395	0.29956	0.71675	mSv
I	2.32712	0.29887	1.31299	mSv
J	1.61784	0.82898	1.22341	mSv
K	1.87699	0.44399	1.16049	mSv
L	1.47570	0.57226	1.02398	mSv
M	0.65664	1.02270	0.83967	mSv
N	0.33298	0.23005	0.28152	mSv
O	1.66164	0.62248	1.14206	mSv
P	2.65722	1.56220	2.10971	mSv
Q	0.77825	0.83724	0.80774	mSv
R	0.71914	0.81853	0.76883	mSv
S	1.48474	1.28470	1.38472	mSv
T	1.79630	3.57870	2.68750	mSv

The limestone samples were crushed into fine particles, aliquots made and placed on positions iii) and iv) of an environmental Thermo-Luminescence dosimeter (TLD 0011), these aliquots were used as TLD chips and analyzed using a 6600 Harshaw TLD reader.



**Figure 7:** The 6600 Harshaw TLD reader (LHS) and the Thermo-Luminescence dosimeter (TLD 0011) (RHS) with positions iii) and iv) covered with the sample aliquots

The dose results of this aliquots are in Table 4 above and on a bar graphical representation of Figure 8 below. The doses represent the ambient dose equivalents  $H_p^*(10)$  measured from the limestones samples that have been analyzed.

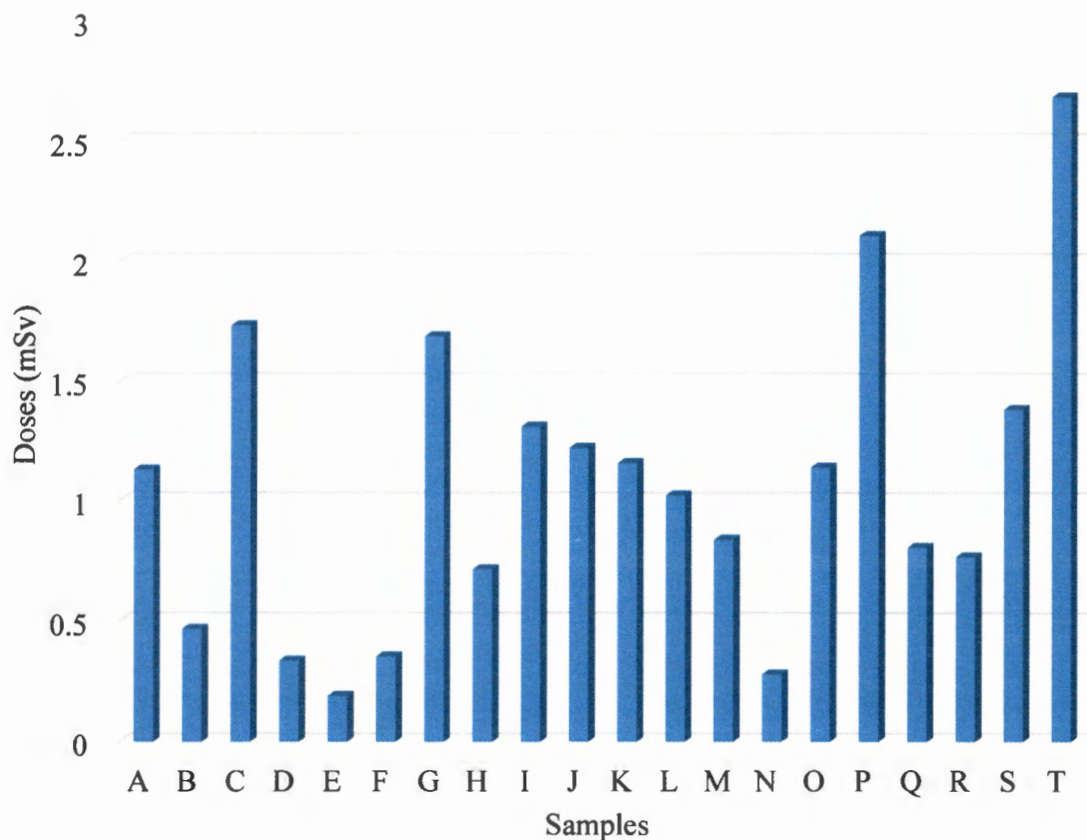


**Figure 8:** Bar chart representation of sample doses from the TLD results

The chart above displays the doses of the samples that were analyzed through thermoluminescence by the use of the Harshaw TLD reader 6600. This chart representation illustrates the correlation of the sample doses, by bestowing the least and highest doses thus also shows that 11 out of the 20 samples were between 1 mSv and 2.7 mSv and only 9 of the 20 samples dose were below 1 mSv. Since these limestones under investigation were mostly used for human shelter construction, the variance in doses may be a result of different times of when the homesteads were formed and other natural events that may have occurred in the past.

The application of an electronic dosimeter in the form of RADEYE was employed to get the dose rates from each of the 20 samples, and the dose rates were comparable. The lowest reading being 0.2  $\mu\text{Sv/hr.}$  and the highest being 0.8  $\mu\text{Sv/hr.}$ , as the results shown in Table 5 and Figure 9 below.

**Table 5:** EPD-RADEYE results for the samples analyzed

SAMPLE ID	A	B	C	D	E	F	G	H	I	J	K	L	M	N	O	P	Q	R	S	T
DOSES ( $\mu\text{Sv/hr.}$ )	0.3	0.4	0.4	0.3	0.4	0.3	0.2	0.3	0.5	0.6	0.4	0.8	0.3	0.8	0.2	0.6	0.5	0.3	0.4	0.3

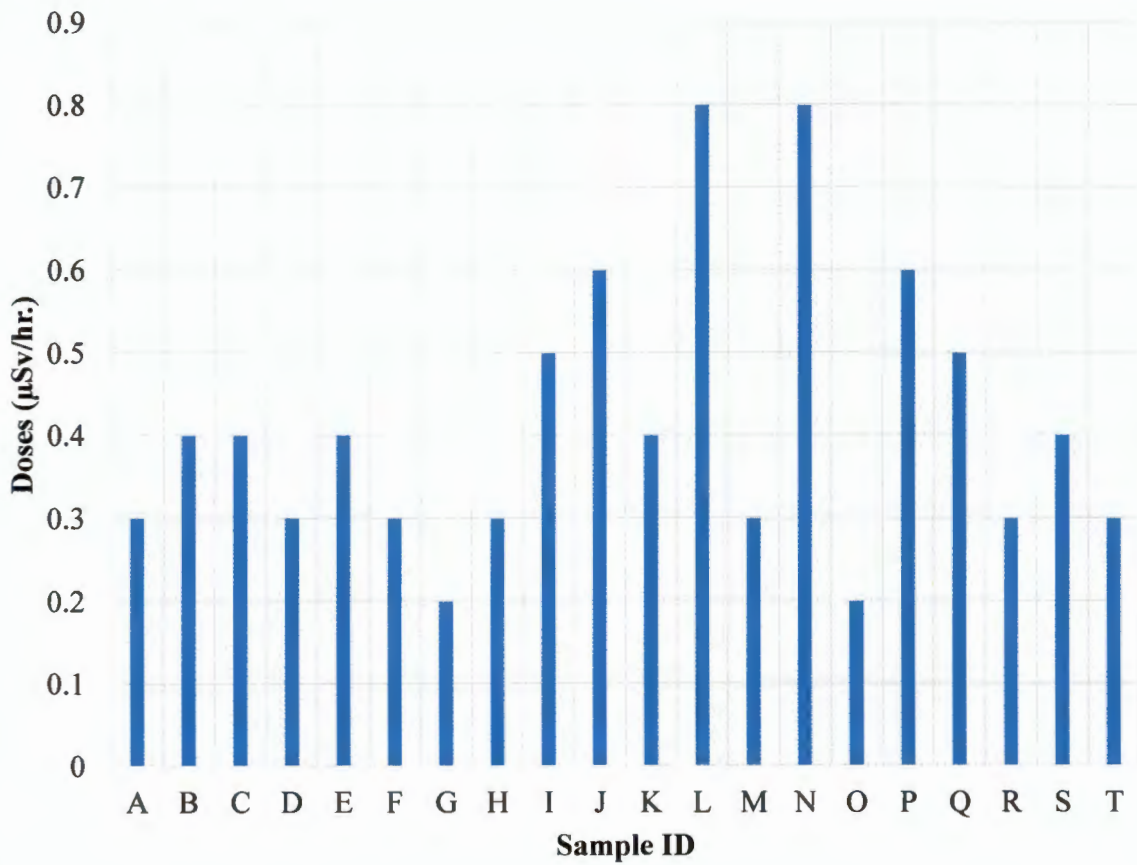


**Figure 9:** Bar chart representation of EPD-RADEYE results analysis for sample doses



The dose rates acquired by the use of an EPD are presented in the chart above on Figure 9, showing the varying dose rates of the samples used for this study, and thus having 14 of the 20 samples being between 0.1 $\mu$ Sv/hr. and 0.4 $\mu$ Sv/hr. Only 6 samples dose rates from the 20 samples were between 0.4 $\mu$ Sv/hr. and 0.8 $\mu$ Sv/hr. And this difference in dose rates of the samples may be as a result of different times of the early settler arrival into this area of Gaborone and other natural activities that may have taken place in the past as the residents of this area relocated to other areas and other new settlers coming in.

### **4.3 Gamma spectrometry results**

To acquire data from the samples collected, the use of High Purity Germanium Well detector resolution (FWHM) (Canberra, United States of America) at 122 keV ( $^{57}\text{Co}$ ) is 0.85 keV and at 1332.5 keV ( $^{60}\text{Co}$ ) is 1.86 keV and relative efficiency for energy 1.33 MeV relative to (NaI) Tl is 36%, (Dlamini et al., 2016).

About 100g of limestone samples were carefully and systematically collected from at least 50 cm deep in each sampling site. In the laboratory, 80g of each sample was measured into the well detector vial. The samples were sealed for 30 days so as to allow for secular equilibrium between Radium-226 ( $^{226}\text{Ra}$ ) and its daughters as well as to prevent radon gas leakage. The samples were measured on the Canberra HPGe well type Detector (Model 747) for 24 hours. Calibration was done by using IAEA Standards (IAEA-35U, 35Th and 35K) with known amount of radioactive elements. Figure 10a and 10b shows the calibration energy and efficiency graphs.

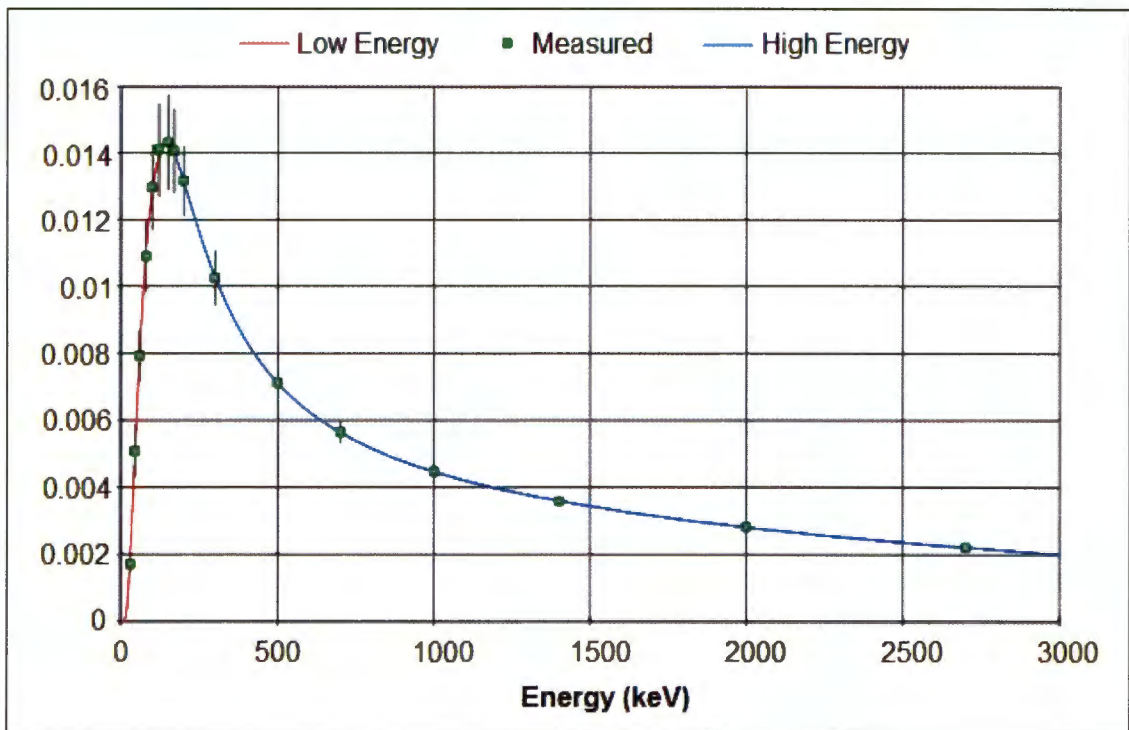


**Figure 10 a):** Efficiency calibration curve for the HPGe well detector

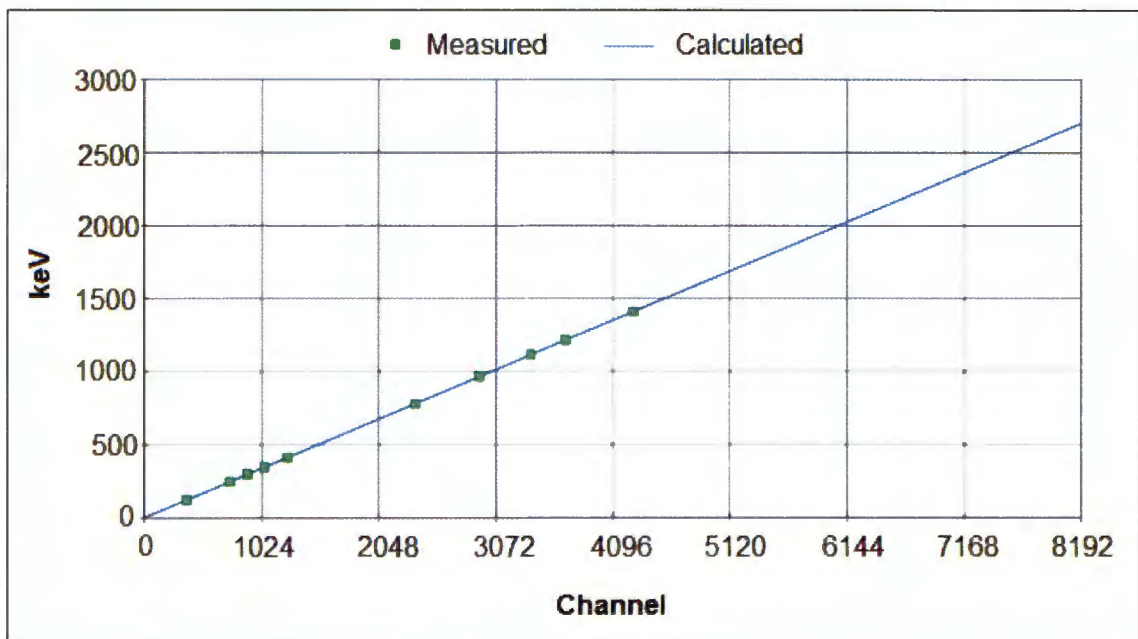


**Figure 10 b):** Energy calibration curve

The limestone samples were run on a Gamma Spectrometer for 24 hours (86400 seconds) in order to acquire the nuclides present on each of the samples. All the sample results were of acceptable expected outcome as the nuclides detected are the daughters of uranium thus enabling the dating of limestones using uranium series and the isotopic ratio a possibility for this research. The activity (Bq) from the gamma ray spectrometer readout has been converted to dose-rate (mSv/hr.) and dose (mSv) by the use of radprocalculator from the website (<http://www.radprocalculator.com/gammer.aspx>) opened on 10/10/2016.

It is noted that the results obtained for the samples through the use of the Gamma Spectrometer are almost similar to the ones found under National Aeronautics and Space Administration (NASA), ([www.mcf.gsfc.nasa.gov](http://www.mcf.gsfc.nasa.gov)) and ([www.-nds.iaea.or.at](http://www.nds.iaea.or.at)). This similarity of the results is an indication that the results for this research are credible. The analysis of results from the Gamma spectrometer for the 20 samples is in Table 6 to 25 showing nuclide identification report.

**Table 6: Nuclide identification report from gamma spectrum analysis for sample A**

Nuclides Identification Report							
Sample ID	Nuclide Name	ID Confidence	Energy (KeV)	Yield (%)	Activity (Bq)	Activity Uncertainty	Dose (mSv)
A	K-40	0.998	1460.81	10.67	9.22E+04	2.74E+03	1.16E+01
	Zn-65	0.998	1115.52	50.75	3.62E+04	7.17E+02	4.55E+00
	Kr-85	0.858	513.99	0.43	8.56E+05	3.56E+04	1.08E+02
	Sr-85	0.842	513.99	99.27	1.39E+04	5.77E+02	1.75E+00
	Cd-109	0.990	88.03	3.72	1.50E+04	1.53E+03	1.88E+00
	Ce-141	0.887	145.44	48.40	3.35E+03	1.28E+03	4.22E-01
	Bi-211	0.316	351.10	12.20	2.31E+04	9.48E+02	2.91E+00
	Bi-212	0.571	727.17	11.80	1.70E+03	6.79E+02	2.14E-01
	Pb-212	0.722	77.11	17.50	1.46E+04	1.64E+03	1.84E+00
			87.20	6.30	7.32E+03	7.16E+02	9.22E-01
			238.63	44.60	1.72E+03	9.93E+01	2.17E-01
	Bi-214	0.719	609.31	46.30	4.57E+03	2.67E+02	5.75E-01
			1120.29	15.10	5.68E+03	4.64E+02	7.15E-01
			1238.11	5.94	4.28E+03	1.46E+03	5.39E-01
			1377.67	4.11	1.49E+04	2.70E+03	1.88E+00
			1729.60	3.05	1.84E+04	3.78E+03	2.32E+00
			1764.49	15.80	1.00E+04	9.57E+02	1.26E+00
			1847.44	2.12	2.21E+04	5.24E+03	2.78E+00
	Pb-214	0.848	77.11	10.70	2.40E+04	2.68E+03	3.02E+00
			87.20	3.70	1.25E+04	1.22E+03	1.57E+00
			241.98	7.49	7.74E+03	5.23E+02	9.75E-01
			295.21	19.20	7.71E+03	4.51E+02	9.71E-01
			351.92	37.20	7.58E+03	3.11E+02	9.54E-01
	Ra-226	0.999	186.21	3.28	2.93E+04	2.24E+03	3.68E+00
	Th-231	0.840	84.21	8.00	1.36E+03	4.46E+02	1.71E-01
			89.95	1.25	3.69E+04	3.61E+03	4.65E+00
	U-235	0.744	89.96	1.50	3.07E+04	3.01E+03	3.86E+00
			93.35	2.50	4.21E+04	2.44E+03	5.30E+00
143.76			10.50	1.06E+03	4.14E+02	1.34E-01	
185.71			54.00	1.78E+03	1.39E+02	2.24E-01	
<b>Average Dose</b>							<b>5.65E+00</b>

**Table 7: Nuclide identification report from gamma spectrum analysis for sample B**

Nuclides Identification Report							
Sample ID	Nuclide Name	ID confidence	Energy (KeV)	Yield (%)	Activity (Bq)	Activity Uncertainty	Dose (mSv)
B	K-40	0.990	1460.81	10.67	1.23E+05	4.24E+03	1.54E+01
	Zn-65	0.996	1115.52	50.75	6.09E+04	1.19E+03	7.67E+00
	Cd-109	0.906	88.03	3.72	1.70E+04	1.91E+03	2.14E+00
	Pb-212	0.926	74.81	9.60	1.46E+04	1.87E+03	1.84E+00
			77.11	17.50	1.17E+04	1.26E+03	1.47E+00
			87.20	6.30	9.23E+03	9.99E+02	1.16E+00
			89.80	1.75	9.57E+03	2.66E+03	1.20E+00
			238.63	44.60	1.99E+03	1.44E+02	2.50E-01
	Bi-214	0.645	609.31	46.30	9.95E+03	4.64E+02	1.25E+00
			1120.29	15.10	7.14E+03	7.16E+02	8.99E-01
			1407.98	2.48	7.81E+03	4.76E+03	9.83E-01
			1509.19	2.19	1.23E+04	3.24E+03	1.54E+00
			1729.60	3.05	2.53E+04	5.98E+03	3.18E+00
			1764.49	15.80	1.33E+04	1.43E+03	1.67E+00
			1847.44	2.12	1.41E+04	6.06E+03	1.78E+00
	Pb-214	0.848	74.81	6.33	2.22E+04	2.883E	2.79E+00
			77.11	10.70	2.40E+04	2.88E+03	3.02E+00
			87.20	3.70	1.25E+04	1.22E+03	1.57E+00
			241.98	7.49	7.74E+03	5.23E+02	9.75E-01
			295.21	19.20	7.71E+03	4.51E+02	9.71E-01
			351.92	37.20	7.58E+03	3.11E+02	9.54E-01
	Ra-226	0.989	186.21	3.28	2.93E+04	2.89E+03	3.68E+00
	Th-231	0.997	84.21	8.00	3.32E+03	6.72E+02	4.18E-01
			89.95	1.25	1.34E+04	3.72E+03	1.69E+00
	U-235	0.523	89.96	1.50	1.12E+04	3.10E+03	1.40E+00
			93.35	2.50	4.03E+04	2.88E+03	5.07E+00
			185.71	54.00	1.80E+03	1.78E+02	2.26E-01
	Average Dose						

**Table 8: Nuclide identification report from gamma spectrum analysis for sample C**

Nuclides Identification Report							
Sample ID	Nuclide Name	ID Confidence	Energy (KeV)	Yield (%)	Activity (Bq)	Activity Uncertainty	Dose (mSv)
C	K-40	0.990	1460.81	10.67	1.23E+05	4.24E+03	1.54E+01
	Zn-65	0.996	1115.52	50.75	6.09E+04	1.19E+03	7.67E+00
	Cd-109	0.906	88.03	3.72	1.70E+04	1.91E+03	2.14E+00
	Pb-212	0.926	74.81	9.60	1.46E+04	1.87E+03	1.84E+00
			77.11	17.50	1.17E+04	1.26E+03	1.47E+00
			87.20	6.30	9.23E+03	9.99E+02	1.16E+00
			89.80	1.75	9.57E+03	2.66E+03	1.20E+00
			238.63	44.60	1.99E+03	1.44E+02	2.50E-01
	Bi-214	0.645	609.31	46.30	5.95E+03	4.64E+02	7.50E-01
			1120.29	15.10	7.14E+03	7.16E+02	8.99E-01
			1407.98	2.48	7.81E+03	4.76E+03	9.83E-01
			1509.19	2.19	1.23E+04	3.24E+03	1.54E+00
			1729.60	3.05	2.53E+04	5.98E+03	3.18E+00
			1764.49	15.80	1.33E+04	1.43E+03	1.67E+00
			1847.44	2.12	1.41E+04	6.06E+03	1.78E+00
	Pb-214	0.986	74.81	6.33	2.22E+04	2.883E	2.79E+00
			77.11	10.70	1.91E+04	2.05E+03	2.40E+00
			87.20	3.70	1.57E+04	1.70E+03	1.98E+00
			241.98	7.49	8.38E+03	7.54E+02	1.06E+00
			295.21	19.20	9.18E+03	6.52E+02	1.16E+00
			351.92	37.20	9.37E+03	4.49E+02	1.18E+00
	Ra-226	0.989	186.21	3.28	2.96E+04	2.89E+03	3.72E+00
	Th-231	0.997	84.21	8.00	3.32E+03	6.72E+02	4.18E-01
			89.95	1.25	1.34E+04	3.72E+03	1.69E+00
	U-235	0.523	89.96	1.50	1.12E+04	3.10E+03	1.40E+00
			93.35	2.50	4.03E+04	2.88E+03	5.07E+00
			185.71	54.00	1.80E+03	1.78E+02	2.26E-01
Average Dose							2.41E+00

**Table 9:** Nuclide identification report from gamma spectrum analysis for sample D

Nuclides Identification Report							
Sample ID	Nuclide Name	ID Confidence	Energy (KeV)	Yield (%)	Activity (Bq)	Activity Uncertainty	Dose (mSv)
D	K-40	1.000	1460.81	10.67	1.29E+05	3.34E+03	1.62E+01
	Zn-65	0.998	1115.52	50.75	3.50E+04	7.15E+02	4.40E+00
	Cd-109	0.986	88.03	3.72	8.99E+03	1.29E+03	1.13E+00
	Ce-141	0.867	145.44	48.40	5.20E+03	2.05E+03	6.55E-01
	Bi-211	0.317	351.10	12.20	1.20E+04	7.76E+02	1.50E+00
	Bi-212	0.570	727.17	11.80	2.68E+03	6.84E+02	3.38E-01
	Pb-212	0.722	77.11	17.50	8.43E+03	1.09E+03	1.06E+00
			87.20	6.30	4.32E+03	6.08E+02	5.44E-01
			238.63	44.60	1.77E+03	1.02E+02	2.23E-01
	Bi-214	0.719	609.31	46.30	2.78E+03	2.81E+02	3.49E-01
			1120.29	15.10	3.81E+03	4.28E+02	4.79E-01
			1377.67	4.11	5.48E+03	2.43E+03	6.90E-01
			1729.60	3.05	8.78E+03	3.53E+03	1.11E+00
			1764.49	15.80	5.79E+03	8.55E+02	7.29E-01
	Pb-214	0.848	77.11	10.70	1.38E+04	1.78E+03	1.74E+00
			87.20	3.70	7.36E+03	1.04E+03	9.27E-01
			241.98	7.49	4.02E+03	4.36E+02	5.06E-01
			295.21	19.20	4.45E+03	3.71E+02	5.61E-01
			351.92	37.20	3.92E+03	2.55E+02	4.93E-01
	Ra-226	0.998	186.21	3.28	2.41E+04	2.15E+03	3.04E+00
	Th-231	0.797	84.21	8.00	3.40E+03	4.79E+02	4.29E-01
			89.95	1.25	8.13E+04	4.80E+03	1.02E+01
	Pa-234M	0.544	1001.03	0.84	1.72E+04	9.76E+03	2.17E+00
	U-235	0.744	93.35	2.50	4.06E+04	2.40E+03	5.11E+00
			143.76	10.50	1.27E+03	5.11E+02	1.60E-01
			185.71	54.00	1.47E+03	1.33E+02	1.84E-01
	Average Dose						

**Table 10:** Nuclide identification report from gamma spectrum analysis for sample E

Nuclides Identification Report							
Sample ID	Nuclide Name	ID Confidence	Energy (KeV)	Yield (%)	Activity (Bq)	Activity Uncertainty	Dose (mSv)
E	K-40	1.000	1460.81	10.67	1.05E+05	2.92E+03	1.33E+01
	Zn-65	0.999	1115.52	50.75	3.35E+04	6.95E+02	4.21E+00
	Cd-109	0.986	88.03	3.72	1.16E+04	1.36E+03	1.46E+00
	Bi-211	0.317	351.10	12.20	1.67E+04	8.48E+02	2.10E+00
	Bi-212	0.571	727.17	11.80	1.12E+03	5.65E+02	1.40E-01
	Pb-212	0.722	77.11	17.50	1.10E+04	1.28E+03	1.39E+00
			87.20	6.30	5.62E+03	6.37E+02	7.07E-01
			238.63	44.60	1.58E+03	9.73E+01	1.98E-01
	Bi-214	0.727	609.31	46.30	4.06E+03	2.94E+02	5.11E-01
			1120.29	15.10	3.02E+03	4.29E+02	3.81E-01
			1238.11	5.94	5.28E+03	1.54E+03	6.65E-01
			1729.60	3.05	1.67E+04	3.44E+03	2.10E+00
			1764.49	15.80	7.70E+03	8.89E+02	9.69E-01
			1847.44	2.12	7.84E+03	3.65E+03	9.87E-01
			2118.54	1.21	1.75E+04	6.77E+03	2.20E+00
	Pb-214	0.848	77.11	10.70	1.80E+04	2.10E+03	2.27E+00
			87.20	3.70	9.57E+03	1.09E+03	1.20E+00
			241.98	7.49	5.44E+03	4.80E+02	6.85E-01
			295.21	19.20	5.50E+03	3.93E+02	6.92E-01
			351.92	37.20	5.48E+03	2.78E+02	6.89E-01
	Ra-226	0.999	186.21	3.28	2.25E+04	2.09E+03	2.83E+00
	Th-231	0.797	84.21	8.00	4.42E+03	5.02E+02	5.57E-01
			89.95	1.25	8.50E+04	4.90E+03	1.07E+01
Pa-234M	0.545	1001.03	0.84	1.69E+04	9.78E+03	2.13E+00	
U-235	0.503	93.35	2.50	4.25E+04	2.45E+03	5.35E+00	
		185.71	54.00	1.37E+03	1.29E+02	1.72E-01	
Average Dose							2.25E+00

**Table 11: Nuclide identification report from gamma spectrum analysis for sample F**

Nuclides Identification Report							
Sample ID	Nuclide Name	ID Confidence	Energy (KeV)	Yield (%)	Activity (Bq)	Activity Uncertainty	Dose (mSv)
F	K-40	1.000	1460.81	10.67	1.09E+05	3.09E+03	1.37E+01
	Zn-65	0.998	1115.52	50.75	3.43E+04	7.13E+02	4.32E+00
	Nb-95	0.839	765.79	99.81	4.49E+03	1.45E+03	5.65E-01
	Cd-109	0.987	88.03	3.72	2.86E+04	2.28E+03	3.60E+00
	Bi-211	0.316	351.10	12.20	4.61E+04	1.47E+03	5.81E+00
	Pb-212	0.722	77.11	17.50	2.82E+04	2.90E+03	3.55E+00
			87.20	6.30	1.39E+04	1.03E+03	1.74E+00
			238.63	44.60	1.56E+03	9.68E+01	1.97E-01
	Bi-214	0.803	609.31	46.30	8.79E+03	3.54E+02	1.11E+00
			768.36	5.04	6.43E+03	2.07E+03	8.09E-01
			1120.29	15.10	8.57E+03	5.73E+02	1.08E+00
			1238.11	5.94	1.26E+04	2.44E+03	1.58E+00
			1377.67	4.11	1.74E+04	2.90E+03	2.19E+00
			1407.98	2.48	1.21E+04	4.92E+03	1.52E+00
			1729.60	3.05	3.11E+04	4.69E+03	3.91E+00
			1764.49	15.80	1.79E+04	1.15E+03	2.25E+00
	Pb-214	0.861	77.11	10.70	4.61E+04	4.75E+03	5.80E+00
			87.20	3.70	2.36E+04	1.75E+03	2.97E+00
			241.98	7.49	1.49E+04	7.27E+02	1.88E+00
			295.21	19.20	1.59E+04	6.61E+02	2.00E+00
			351.92	37.20	1.51E+04	4.83E+02	1.90E+00
			785.91	1.10	3.90E+04	1.07E+04	4.91E+00
	Ra-226	0.999	186.21	3.28	4.37E+04	2.58E+03	5.50E+00
	Th-231	0.840	84.21	8.00	4.57E+03	5.80E+02	5.75E-01
			89.95	1.25	1.09E+05	5.83E+03	1.37E+01
	Pa-234M	0.983	766.36	0.29	1.10E+05	3.55E+04	1.39E+01
			1001.03	0.84	3.08E+04	1.17E+04	3.88E+00
U-235	0.503	93.35	2.50	5.43E+04	2.92E+03	6.83E+00	
		185.71	54.00	2.65E+03	1.62E+02	3.34E-01	
<b>Average Dose</b>							<b>3.86E+00</b>

**Table 12: Nuclide identification report from gamma spectrum analysis for sample G**

Nuclides Identification Report							
Sample ID	Nuclide Name	ID Confidence	Energy (KeV)	Yield (%)	Activity (Bq)	Activity Uncertainty	Dose (mSv)
G	K-40	1.000	1460.81	10.67	1.12E+05	3.17E+03	1.41E+01
	Zn-65	0.998	1115.52	50.75	3.48E+04	7.24E+02	4.38E+00
	Nb-95	0.825	765.79	99.81	1.09E+04	2.23E+03	1.37E+00
	Cd-109	0.988	88.03	3.72	3.79E+04	2.82E+03	4.76E+00
	Ce-141	0.881	145.44	48.40	6.72E+03	1.09E+03	8.45E-01
	Bi-211	0.317	351.10	12.20	7.07E+04	2.01E+03	8.90E+00
	Pb-212	0.722	77.11	17.50	4.30E+04	4.36E+03	5.41E+00
			87.20	6.30	1.82E+04	1.25E+03	2.29E+00
			238.63	44.60	1.88E+03	1.05E+02	2.37E-01
	Bi-214	0.865	609.31	46.30	1.32E+04	4.66E+02	1.66E+00
			768.36	5.04	1.45E+04	2.96E+03	1.82E+00
			934.06	3.21	1.04E+04	3.27E+03	1.30E+00
			1120.29	15.10	1.23E+04	6.74E+02	1.54E+00
			1238.11	5.94	9.93E+03	2.57E+03	1.25E+00
			1377.67	4.11	3.32E+04	3.31E+03	4.18E+00
			1509.19	2.19	8.61E+03	4.31E+03	1.08E+00
			1729.60	3.05	4.99E+04	5.51E+03	6.28E+00
			1764.49	15.80	2.82E+04	1.49E+03	3.55E+00
	Pb-214	0.848	1847.44	2.12	3.54E+04	6.50E+03	4.45E+00
			77.11	10.70	7.04E+04	7.13E+03	8.86E+00
			87.20	3.70	3.11E+04	2.12E+03	3.91E+00
			241.98	7.49	2.31E+04	9.47E+02	2.90E+00
			295.21	19.20	2.33E+04	8.44E+02	2.93E+00
	Ra-226	0.999	351.92	37.20	2.32E+04	6.60E+02	2.92E+00
			186.21	3.28	5.66E+04	2.78E+03	7.13E+00
	Th-231	0.840	84.21	8.00	4.86E+03	6.15E+02	6.12E-01
			89.95	1.25	1.34E+05	6.83E+03	1.69E+01
	Pa-234M	0.981	766.36	0.29	2.48E+05	5.07E+04	3.12E+01
			1001.03	0.84	4.85E+04	1.25E+04	6.10E+00
	U-235	0.718	93.35	2.50	6.72E+04	3.42E+03	8.46E+00
			143.76	10.50	1.68E+03	3.00E+02	2.11E-01
			185.71	54.00	3.44E+03	1.78E+02	4.33E-01
<b>Average Dose</b>							<b>5.06E+00</b>

**Table 13: Nuclide identification report from gamma spectrum analysis for sample H**

Nuclides Identification Report							
Sample ID	Nuclide Name	ID Confidence	Energy (KeV)	Yield (%)	Activity (Bq)	Activity Uncertainty	Dose (mSv)
H	K-40	1.000	1460.81	10.67	1.12E+05	3.17E+03	1.41E+01
	Zn-65	0.998	1115.52	50.75	3.48E+04	7.24E+02	4.38E+00
	Nb-95	0.825	765.79	99.81	1.09E+04	2.23E+03	1.37E+00
	Cd-109	0.988	88.03	3.72	3.79E+04	2.82E+03	4.76E+00
	Ce-141	0.881	145.44	48.40	6.72E+03	1.09E+03	8.45E-01
	Bi-211	0.317	351.10	12.20	7.07E+04	2.01E+03	8.90E+00
	Pb-212	0.722	77.11	17.50	4.30E+04	4.36E+03	5.41E+00
			87.20	6.30	1.82E+04	1.25E+03	2.29E+00
			238.63	44.60	1.88E+03	1.05E+02	2.37E-01
	Bi-214	0.865	609.31	46.30	1.32E+04	4.66E+02	1.66E+00
			768.36	5.04	1.45E+04	2.96E+03	1.82E+00
			934.06	3.21	1.04E+04	3.27E+03	1.30E+00
			1120.29	15.10	1.23E+04	6.74E+02	1.54E+00
			1238.11	5.94	9.93E+03	2.57E+03	1.25E+00
			1377.67	4.11	3.32E+04	3.31E+03	4.18E+00
			1509.19	2.19	8.61E+03	4.31E+03	1.08E+00
			1729.60	3.05	4.99E+04	5.51E+03	6.28E+00
			1764.49	15.80	2.82E+04	1.49E+03	3.55E+00
			1847.44	2.12	3.54E+04	6.50E+03	4.45E+00
	Pb-214	0.848	77.11	10.70	7.04E+04	7.13E+03	8.86E+00
			87.20	3.70	3.11E+04	2.12E+03	3.91E+00
			241.98	7.49	2.31E+04	9.47E+02	2.90E+00
			295.21	19.20	2.33E+04	8.44E+02	2.93E+00
			351.92	37.20	2.32E+04	6.60E+02	2.92E+00
	Ra-226	0.999	186.21	3.28	5.66E+04	2.78E+03	7.13E+00
	Th-231	0.840	84.21	8.00	4.86E+03	6.15E+02	6.12E-01
			89.95	1.25	1.34E+05	6.83E+03	1.69E+01
	Pa-234M	0.981	766.36	0.29	2.48E+05	5.07E+04	3.12E+01
			1001.03	0.84	4.85E+04	1.25E+04	6.10E+00
	U-235	0.718	93.35	2.50	6.72E+04	3.42E+03	8.46E+00
143.76			10.50	1.68E+03	3.00E+02	2.11E-01	
185.71			54.00	3.44E+03	1.78E+02	4.33E-01	
<b>Average Dose</b>							<b>5.06E+00</b>

**Table 14:** Nuclide identification report from gamma spectrum analysis for sample I

Nuclides Identification Report							
Sample ID	Nuclide Name	ID Confidence	Energy (KeV)	Yield (%)	Activity (Bq)	Activity Uncertainty	Dose (mSv)
I	K-40	1.000	1460.81	10.67	9.67E+04	2.79E+03	1.22E+01
	Zn-65	0.999	1115.52	50.75	3.52E+04	7.09E+02	4.43E+00
	Cd-109	0.990	88.03	3.72	1.17E+04	1.38E+03	1.47E+00
	Bi-211	0.316	351.10	12.20	1.73E+04	8.32E+02	2.18E+00
	Pb-212	0.722	77.11	17.50	1.22E+04	1.38E+03	1.54E+00
			87.20	6.30	5.72E+03	6.50E+02	7.19E-01
			238.63	44.60	2.00E+03	1.08E+02	2.52E-01
	Bi-214	0.646	609.31	46.30	3.79E+03	2.96E+02	4.76E-01
			1120.29	15.10	3.75E+03	4.19E+02	4.72E-01
			1377.67	4.11	5.14E+03	1.96E+03	6.48E-01
			1729.60	3.05	1.10E+04	3.59E+03	1.39E+00
			1764.49	15.80	8.55E+03	8.98E+02	1.08E+00
			1847.44	2.12	1.00E+04	4.28E+03	1.26E+00
	Pb-214	0.848	77.11	10.70	2.00E+04	2.25E+03	2.52E+00
			87.20	3.70	9.73E+03	1.11E+03	1.23E+00
			241.98	7.49	7.22E+03	5.08E+02	9.09E-01
			295.21	19.20	6.40E+03	4.17E+02	8.05E-01
			351.92	37.20	5.68E+03	2.73E+02	7.15E-01
	Ra-226	0.998	186.21	3.28	2.42E+04	1.97E+03	3.05E+00
	U-235	0.529	89.96	1.50	2.40E+04	2.73E+03	3.02E+00
			93.35	2.50	4.15E+04	2.41E+03	5.22E+00
			185.71	54.00	1.47E+03	1.22E+02	1.85E-01
	Average Dose						

**Table 15: Nuclide identification report from gamma spectrum analysis for sample J**

Nuclides Identification Report							
Sample ID	Nuclide Name	ID Confidence	Energy (KeV)	Yield (%)	Activity (Bq)	Activity Uncertainty	Dose (mSv)
J	K-40	1.000	1460.81	10.67	9.67E+04	2.79E+03	1.22E+01
	Zn-65	0.999	1115.52	50.75	3.52E+04	7.09E+02	4.43E+00
	Cd-109	0.990	88.03	3.72	1.17E+04	1.38E+03	1.47E+00
	Bi-211	0.316	351.10	12.20	1.73E+04	8.32E+02	2.18E+00
	Pb-212	0.722	77.11	17.50	1.22E+04	1.38E+03	1.54E+00
			87.20	6.30	5.72E+03	6.50E+02	7.19E-01
			238.63	44.60	2.00E+03	1.08E+02	2.52E-01
	Bi-214	0.646	609.31	46.30	3.79E+03	2.96E+02	4.76E-01
			1120.29	15.10	3.75E+03	4.19E+02	4.72E-01
			1377.67	4.11	5.14E+03	1.96E+03	6.48E-01
			1729.60	3.05	1.10E+04	3.59E+03	1.39E+00
			1764.49	15.80	8.55E+03	8.98E+02	1.08E+00
	Pb-214	0.848	1847.44	2.12	1.00E+04	4.28E+03	1.26E+00
			77.11	10.70	2.00E+04	2.25E+03	2.52E+00
			87.20	3.70	9.73E+03	1.11E+03	1.23E+00
			241.98	7.49	7.22E+03	5.08E+02	9.09E-01
			295.21	19.20	6.40E+03	4.17E+02	8.05E-01
	Ra-226	0.998	351.92	37.20	5.68E+03	2.73E+02	7.15E-01
			186.21	3.28	2.42E+04	1.97E+03	3.05E+00
	U-235	0.529	89.96	1.50	2.40E+04	2.73E+03	3.02E+00
			93.35	2.50	4.15E+04	2.41E+03	5.22E+00
185.71			54.00	1.47E+03	1.22E+02	1.85E-01	
<b>Average Dose</b>							<b>2.08E+00</b>

**Table 16:** Nuclide identification report from gamma spectrum analysis for sample K

Nuclides Identification Report							
Sample ID	Nuclide Name	ID Confidence	Energy (KeV)	Yield (%)	Activity (Bq)	Activity Uncertainty	Dose (mSv)
K	K-40	1.000	1460.81	10.67	1.13E+05	3.06E+03	1.43E+01
	Zn-65	0.998	1115.52	50.75	3.50E+04	7.17E+02	4.41E+00
	Cd-109	0.989	88.03	3.72	1.10E+04	1.36E+03	1.38E+00
	Bi-211	0.317	351.10	12.20	2.15E+04	9.61E+02	2.71E+00
	Pb-212	0.722	77.11	17.50	1.54E+04	1.69E+03	1.93E+00
			87.20	6.30	5.29E+03	6.37E+02	6.66E-01
			238.63	44.60	2.16E+03	1.11E+02	2.72E-01
	Bi-214	0.625	609.31	46.30	4.39E+03	3.00E+02	5.52E-01
			1120.29	15.10	4.04E+03	4.68E+02	5.09E-01
			1377.67	4.11	7.55E+03	2.37E+02	9.50E-01
			1729.60	3.05	1.43E+04	4.28E+03	1.81E+00
			1764.49	15.80	9.96E+03	9.93E+02	1.25E+00
	Pb-214	0.848	77.11	10.70	2.51E+04	2.77E+03	3.16E+00
			87.20	3.70	9.01E+03	1.09E+03	1.13E+00
			241.98	7.49	8.42E+03	5.46E+02	1.06E+00
			295.21	19.20	7.25E+03	4.75E+02	9.12E-01
			351.92	37.20	7.06E+03	3.15E+02	8.88E-01
	Ra-226	0.998	186.21	3.28	2.54E+04	2.22E+03	3.20E+00
	U-235	0.529	93.35	2.50	3.61E+04	2.24E+03	4.54E+00
			185.71	54.00	1.55E+03	1.37E+02	1.94E-01
	<b>Average Dose</b>						



**Table 17: Nuclide identification report from gamma spectrum analysis for sample L**

<b>Nuclear Identification Report</b>							
<b>Sample ID</b>	<b>Nuclide Name</b>	<b>ID Confidence</b>	<b>Energy (KeV)</b>	<b>Yield (%)</b>	<b>Activity (Bq)</b>	<b>Activity Uncertainty</b>	<b>Dose (mSv)</b>
<b>L</b>	<b>K-40</b>	1.000	1460.81	10.67	1.41E+05	3.57E+03	1.78E+01
	<b>Zn-65</b>	0.998	1115.52	50.75	3.44E+04	7.14E+02	4.33E+00
	<b>Bi-211</b>	0.316	351.10	12.20	1.34E+04	7.51E+02	1.68E+00
	<b>Pb-212</b>	0.629	77.11	17.50	7.93E+03	1.04E+03	9.98E-01
			89.80	1.75	5.86E+04	4.39E+03	7.38E+00
			238.63	44.60	1.76E+03	1.01E+02	2.21E-01
	<b>Bi-214</b>	0.577	609.31	46.30	2.66E+03	2.39E+02	3.34E-01
			1120.29	15.10	2.21E+03	4.20E+02	2.78E-01
			1729.60	3.05	1.23E+04	3.12E+03	1.54E+00
			1764.49	15.80	7.31E+03	8.39E+02	9.20E-01
	<b>Pb-214</b>	0.791	77.11	10.70	1.30E+04	1.70E+03	1.63E+00
			89.80	1.03	9.96E+04	7.46E+03	1.25E+01
			241.98	7.49	4.92E+03	4.53E+02	6.20E-01
			295.21	19.20	4.49E+03	4.08E+02	5.65E-01
			351.92	37.20	4.39E+03	2.46E+02	5.52E-01
	<b>Ra-226</b>	0.997	186.21	3.28	1.93E+04	1.94E+03	2.43E+00
	<b>Ac-228</b>	0.308	93.35	3.50	2.93E+04	2.20E+03	3.69E+00
			338.32	11.4	1.18E+03	5.07E+02	1.48E-01
			911.6	27.70	2.17E+03	4.92E+02	2.73E-01
			969.11	16.6	1.20E+03	4.85E+02	1.50E-01
<b>Pa-234M</b>	0.544	1001.03	0.84	2.07E+04	1.02E+04	2.60E+00	
<b>U-235</b>	0.504	93.35	2.50	4.10E+04	3.07E+03	5.16E+00	
		185.71	54.00	1.17E+03	1.19E+02	1.47E-01	
<b>Average Dose</b>							<b>2.87E+00</b>

**Table 18: Nuclide identification report from gamma spectrum analysis for sample M**

Nuclides Identification Report							
Sample ID	Nuclide Name	ID Confidence	Energy (KeV)	Yield (%)	Activity (Bq)	Activity Uncertainty	Dose (mSv)
M	K-40	1.000	1460.81	10.67	1.07E+05	2.94E+03	1.34E+01
	Zn-65	0.999	1115.52	50.75	3.40E+04	6.98E+03	4.28E+00
	Cd-109	0.988	88.03	3.72	8.77E+03	1.28E+03	1.10E+00
	Bi-211	0.317	351.10	12.20	1.71E+04	8.12E+02	2.15E+00
	Pb-212	0.722	77.11	17.50	1.12E+04	1.33E+03	1.41E+00
			87.20	6.30	4.26E+03	6.07E+02	5.36E-01
			238.63	44.60	1.58E+03	9.65E+01	1.99E-01
	Bi-214	0.688	609.31	46.30	3.56E+03	2.96E+02	4.48E-01
			806.17	1.23	2.32E+04	6.88E+03	2.92E+00
			1120.29	15.10	3.86E+03	4.54E+02	4.86E-01
			1238.11	5.94	2.62E+03	1.60E+03	3.30E-01
			1729.60	3.05	1.13E+04	2.84E+03	1.42E+00
			1764.49	15.80	8.72E+03	9.46E+02	1.10E+00
	Pb-214	0.848	1847.44	2.12	9.47E+03	3.98E+03	1.19E+00
			77.11	10.70	1.84E+04	2.18E+03	2.31E+00
			87.20	3.70	7.26E+03	1.03E+03	9.14E-01
			241.98	7.49	4.94E+03	4.46E+02	6.22E-01
			295.21	19.20	5.28E+03	4.25E+03	6.64E-01
	Ra-226	0.998	351.92	37.20	5.61E+03	2.67E+02	7.06E-01
			186.21	3.28	2.28E+04	1.90E+03	2.87E+00
	Pa-234M	0.545	1001.03	0.84	1.94E+04	1.21E+04	2.44E+00
U-235	0.503	93.35	2.50	3.97E+04	2.37E+03	4.99E+00	
		185.71	54.00	1.38E+03	1.17E+02	1.74E-01	
Average Dose							2.03E+00

**Table 19: Nuclide identification report from gamma spectrum analysis for sample N**

Nuclides Identification Report							
Sample ID	Nuclide Name	ID Confidence	Energy (KeV)	Yield (%)	Activity (Bq)	Activity Uncertainty	Dose (mSv)
N	K-40	1.000	1460.81	10.67	1.23E+05	3.27E+03	1.55E+01
	Zn-65	0.999	1115.52	50.75	3.44E+04	8.22E+02	4.33E+00
	Cd-109	0.985	88.03	3.72	5.51E+03	1.15E+03	6.94E-01
	Ce-141	0.883	145.44	48.40	2.45E+03	1.35E+03	3.08E-01
	Bi-211	0.317	351.10	12.20	1.27E+04	7.04E+02	1.60E+00
	Pb-212	0.722	77.11	17.50	1.04E+04	1.24E+03	1.30E+00
			87.20	6.30	2.69E+03	5.55E+02	3.38E-01
			238.63	44.60	1.72E+03	9.98E+01	2.17E-01
	Bi-214	0.352	609.31	46.30	3.07E+03	2.79E+02	3.87E-01
			1764.49	15.80	6.87E+03	8.12E+02	8.64E-01
	Pb-214	0.848	77.11	10.70	1.69E+04	2.03E+03	2.13E+00
			87.20	3.70	4.58E+03	9.46E+02	5.76E-01
			241.98	7.49	4.46E+03	4.51E+02	5.62E-01
			295.21	19.20	4.45E+03	3.77E+02	5.60E-01
			351.92	37.20	4.16E+03	2.31E+02	5.24E-01
	Ra-226	0.997	186.21	3.28	2.14E+04	1.77E+03	2.70E+00
	Th-231	0.840	84.21	8.00	1.53E+03	4.11E+02	1.92E-01
			89.95	1.25	6.95E+04	6.43E+03	8.75E+00
	Pa-234M	0.544	1001.03	0.84	4.80E+04	1.62E+04	6.04E+00
	U-235	0.719	93.35	2.50	3.48E+04	3.21E+03	4.37E+00
143.76			10.50	7.26E+02	4.04E+02	9.14E-02	
185.71			54.00	1.30E+03	1.09E+02	1.64E-01	
<b>Average Dose</b>							<b>2.37E+00</b>

**Table 20: Nuclide identification report from gamma spectrum analysis for sample O**

Nuclides Identification Report							
Sample ID	Nuclide Name	ID Confidence	Energy (KeV)	Yield (%)	Activity (Bq)	Activity Uncertainty	Dose (mSv)
O	K-40	0.999	1460.81	10.67	1.03E+05	2.92E+03	1.29E+01
	Zn-65	0.998	1115.52	50.75	3.58E+04	7.21E+02	4.51E+00
	Cd-109	0.986	88.03	3.72	1.38E+04	1.52E+03	1.73E+00
	Bi-211	0.318	351.10	12.20	2.17E+04	9.62E+02	2.73E+00
	Pb-212	0.722	77.11	17.50	1.56E+04	1.71E+03	1.96E+00
			87.20	6.30	6.70E+03	7.10E+02	8.43E-01
			238.63	44.60	1.97E+03	1.07E+02	2.49E-01
	Bi-214	0.708	609.31	46.30	4.28E+03	2.93E+02	5.39E-01
			1120.29	15.10	4.24E+03	4.43E+02	5.33E-01
			1238.11	5.94	4.22E+03	1.79E+03	5.31E-01
			1377.67	4.11	7.90E+03	2.02E+03	9.94E-01
			1729.60	3.05	1.69E+04	3.36E+03	2.12E+00
			1764.49	15.80	9.52E+03	9.06E+02	1.20E+00
			2118.54	1.21	1.43E+04	6.04E+03	1.80E+00
	Pb-214	0.848	77.11	10.70	2.55E+04	2.79E+03	3.20E+00
			87.2	3.70	1.14E+04	1.21E+03	1.44E+00
			241.98	7.49	7.30E+03	5.09E+02	9.19E-01
			295.21	19.20	6.34E+03	4.48E+02	7.98E-01
			351.92	37.20	7.10E+03	3.16E+02	8.94E-01
	Ra-226	0.996	186.21	3.28	2.14E+04	1.91E+03	2.70E+00
	Th-231	0.797	84.21	8.00	5.27E+03	5.59E+02	6.64E-01
89.95			1.25	8.22E+04	4.85E+03	1.03E+01	
U-235	0.719	93.35	2.50	4.11E+04	2.42E+03	5.17E+00	
		185.71	54.00	1.47E+03	1.19E+02	1.84E-01	
<b>Average Dose</b>							<b>2.46E+00</b>

**Table 21: Nuclide identification report from gamma spectrum analysis for sample P**

Nuclides Identification Report							
Sample ID	Nuclide Name	ID Confidence	Energy (KeV)	Yield (%)	Activity (Bq)	Activity Uncertainty	Dose (mSv)
P	K-40	1.000	1460.81	10.67	1.16E+05	3.14E+03	1.46E+01
	Zn-65	0.998	1115.52	50.75	3.64E+04	7.37E+02	4.59E+00
	Bi-211	0.316	351.10	12.20	1.56E+04	7.88E+02	1.97E+00
	Bi-212	0.571	727.17	11.80	2.38E+03	8.38E+02	2.99E-01
	Pb-212	0.629	77.11	17.50	1.11E+04	1.31E+03	1.40E+00
			89.80	1.75	4.97E+04	4.64E+03	6.26E+00
			238.63	44.60	1.84E+03	1.02E+02	2.32E-01
	Bi-214	0.593	609.31	46.30	3.60E+03	2.55E+02	4.54E-01
			1120.29	15.10	4.16E+03	4.34E+02	5.24E-01
			1377.67	4.11	6.75E+03	2.75E+03	8.50E-01
			1764.49	15.80	8.15E+03	8.69E+03	1.03E+00
	Pb-214	0.791	77.11	10.70	1.82E+04	2.13E+03	2.28E+00
			89.8	1.03	8.45E+04	7.88E+03	1.06E+01
			241.98	7.49	5.19E+03	4.60E+03	6.53E-01
			295.21	19.20	4.47E+03	3.87E+02	5.63E-01
			351.92	37.20	5.12E+03	2.59E+02	6.44E-01
	Ra-226	0.998	186.21	3.28	2.45E+04	2.08E+03	3.09E+00
	Pa-234M	0.543	1001.03	0.84	2.66E+04	1.00E+04	3.34E+00
	U-235	0.504	93.35	2.50	3.48E+04	3.24E+03	4.38E+00
			185.71	54.00	1.49E+03	1.28E+02	1.88E-01
<b>Average Dose</b>							<b>2.90E+00</b>

**Table 22:** Nuclide identification report from gamma spectrum analysis for sample Q

Nuclides Identification Report							
Sample ID	Nuclide Name	ID Confidence	Energy (KeV)	Yield (%)	Activity (Bq)	Activity Uncertainty	Dose (mSv)
Q	K-40	1.000	1460.81	10.67	9.67E+04	2.79E+03	1.22E+01
	Zn-65	0.999	1115.52	50.75	3.52E+04	7.09E+02	4.43E+00
	Cd-109	0.990	88.03	3.72	1.17E+04	1.38E+03	1.47E+00
	Bi-211	0.316	351.10	12.20	1.73E+04	8.32E+02	2.18E+00
	Pb-212	0.722	77.11	17.50	1.22E+04	1.38E+03	1.54E+00
			87.20	6.30	5.72E+03	6.50E+02	7.19E-01
			238.63	44.60	2.00E+03	1.08E+02	2.52E-01
	Bi-214	0.646	609.31	46.30	3.79E+03	2.96E+02	4.76E-01
			1120.29	15.10	3.75E+03	4.19E+02	4.72E-01
			1377.67	4.11	5.14E+03	1.96E+03	6.48E-01
			1729.60	3.05	1.10E+04	3.59E+03	1.39E+00
			1764.49	15.80	8.55E+03	8.98E+02	1.08E+00
			1847.44	2.12	1.00E+04	4.28E+03	1.26E+00
	Pb-214	0.848	77.11	10.70	2.00E+04	2.25E+03	2.52E+00
			87.20	3.70	9.73E+03	1.11E+03	1.23E+00
			241.98	7.49	7.22E+03	5.08E+02	9.09E-01
			295.21	19.20	6.40E+03	4.17E+02	8.05E-01
			351.92	37.20	5.68E+03	2.73E+02	7.15E-01
	Ra-226	0.998	186.21	3.28	2.42E+04	1.97E+03	3.05E+00
	U-235	0.529	89.96	1.50	2.40E+04	2.73E+03	3.02E+00
			93.35	2.50	4.15E+04	2.41E+03	5.22E+00
185.71			54.00	1.47E+03	1.22E+02	1.85E-01	
<b>Average Dose</b>							<b>2.08E+00</b>

**NWU  
LIBRARY**

**Table 23: Nuclide identification report from gamma spectrum analysis for sample R**

Nuclides Identification Report							
Sample ID	Nuclide Name	ID Confidence	Energy (KeV)	Yield (%)	Activity (Bq)	Activity Uncertainty	Dose (mSv)
R	K-40	1.000	1460.81	10.67	1.07E+05	3.07E+03	1.34E+01
	Zn-65	0.998	1115.52	50.75	3.41E+04	7.04E+02	4.29E+00
	Cd-109	0.985	88.03	3.72	4.73E+03	1.90E+03	5.95E-01
	Ce-141	0.888	145.44	48.40	5.72E+03	1.03E+03	7.20E-01
	Bi-211	0.317	351.10	12.20	1.78E+04	1.14E+03	2.23E+00
	Pb-212	0.722	77.11	17.50	1.21E+04	1.40E+03	1.52E+00
			87.20	6.30	2.29E+03	9.16E+02	2.88E-01
			238.63	44.60	1.61E+03	9.71E+01	2.03E-01
	Bi-214	0.625	609.31	46.30	3.81E+03	2.92E+02	4.80E-01
			1120.29	15.10	2.83E+03	4.18E+02	3.56E-01
			1377.67	4.11	3.88E+03	2.09E+03	4.89E-01
			1729.60	3.05	1.53E+04	3.38E+03	1.93E+00
			1764.49	15.80	7.18E+03	8.72E+02	9.04E-01
	Pb-214	0.848	77.11	10.70	1.97E+04	2.29E+03	2.48E+00
			87.20	3.70	3.90E+03	1.56E+03	4.90E-01
			241.98	7.49	6.26E+03	4.84E+02	7.87E-01
			295.21	19.20	6.27E+03	4.54E+02	7.89E-01
			351.92	37.20	5.82E+03	3.73E+03	7.33E-01
	Ra-226	0.998	186.21	3.28	2.28E+04	2.19E+03	2.87E+00
	Th-231	0.797	84.21	8.00	1.80E+03	7.21E+02	2.27E-01
			89.95	1.25	6.42E+04	5.80E+03	8.08E+00
	U-235	0.719	93.35	2.50	3.21E+04	2.90E+03	4.04E+00
			143.76	10.50	1.52E+03	2.96E+02	1.91E-01
185.71			54.00	1.39E+03	1.35E+02	1.74E-01	
<b>Average Dose</b>							<b>2.01E+00</b>

**Table 24:** Nuclide identification report from gamma spectrum analysis for sample S

Nuclides Identification Report							
Sample ID	Nuclide Name	ID Confidence	Energy (KeV)	Yield (%)	Activity (Bq)	Activity Uncertainty	Dose (mSv)
S	K-40	1.000	1460.81	10.67	9.39E+04	2.86E+03	3.60E-01
	Zn-65	0.999	1115.52	50.75	3.61E+04	7.25E+02	9.12E-02
	Nb-95	0.837	765.79	99.81	8.57E+03	1.61E+03	2.03E-01
	Cd-109	0.989	88.03	3.72	3.94E+04	2.88E+03	3.62E-01
	Xe-131M	0.564	163.93	1.96	5.90E+06	3.15E+06	3.97E+02
	Ce-141	0.887	165.85	80.35	1.66E+02	8.81E+01	1.11E-02
	Bi-211	0.317	351.10	12.20	6.94E+04	2.01E+03	2.53E-01
	Pb-212	0.722	77.11	17.50	4.16E+04	4.21E+03	5.30E-01
			87.20	6.30	1.93E+04	1.29E+03	1.62E-01
			238.63	44.60	1.51E+03	9.57E+01	1.20E-02
	Bi-214	0.905	609.31	46.30	1.36E+04	4.70E+02	5.91E-02
			768.36	5.04	1.39E+04	2.62E+03	3.30E-01
			934.06	3.21	1.28E+04	3.62E+03	4.55E-01
			1120.29	15.10	1.10E+04	6.29E+02	7.92E-02
			1238.11	5.94	1.14E+04	2.74E+03	3.45E-01
			1377.67	4.11	2.54E+04	3.01E+03	3.79E-01
			1407.98	2.48	1.10E+04	4.22E+03	5.31E-01
			1509.19	2.19	1.57E+04	4.71E+03	5.93E-01
			1729.60	3.05	4.54E+04	4.96E+03	6.24E-01
			1764.49	15.80	2.42E+04	1.41E+03	1.78E-01
			1847.44	2.12	3.91E+04	6.63E+03	8.34E-01
	2118.54	1.21	2.21E+04	1.00E+04	1.26E+00		
	Pb-214	0.848	77.11	10.70	6.80E+04	6.89E+03	8.67E-01
			87.20	3.70	3.28E+04	2.19E+03	2.76E-01
			241.98	7.49	2.13E+04	8.97E+02	1.13E-01
			295.21	19.20	2.23E+04	7.92E+02	9.98E-02
			351.92	37.20	2.28E+04	6.59E+02	8.29E-02
	Ra-226	0.999	186.21	3.28	5.85E+04	2.70E+03	3.40E-01
	Th-231	0.840	84.21	8.00	4.13E+03	5.80E+02	7.30E-02
			89.95	1.25	1.39E+05	6.93E+03	8.73E-01
	Pa-234M	0.982	766.36	0.29	2.39E+05	4.49E+04	5.65E+00
			1001.03	0.84	3.95E+04	1.28E+04	1.61E+00
	U-235	0.598	93.35	2.50	6.92E+04	3.47E+03	4.36E-01
163.35			4.70	1.50E+03	8.06E+02	1.02E-01	
185.71			54.00	3.55E+03	1.74E+02	2.19E-02	
Average Dose							1.19E+01

**Table 25:** Nuclide identification report from gamma spectrum analysis for sample T

Nuclides Identification Report							
Sample ID	Nuclide Name	ID Confidence	Energy (KeV)	Yield (%)	Activity (Bq)	Activity Uncertainty	Dose (mSv)
T	K-40	0.990	1460.81	10.67	1.23E+05	4.24E+03	1.54E+01
	Zn-65	0.998	1115.52	50.75	6.09E+04	1.19E+03	7.67E+00
	Pb-212	0.926	74.81	9.60	1.46E+04	1.87E+03	1.84E+00
			77.11	17.50	1.17E+04	1.26E+03	1.47E+00
			87.20	6.30	9.23E+03	9.99E+02	1.16E+00
			89.80	1.75	9.57E+03	2.66E+03	1.20E+00
			238.63	44.60	1.99E+03	1.44E+02	2.50E-01
	Bi-214	0.645	609.31	46.30	9.95E+03	4.64E+02	1.25E+00
			1120.29	15.10	7.14E+03	7.16E+02	8.99E-01
			1407.98	2.48	7.81E+03	4.76E+03	9.83E-01
			1509.19	2.19	1.23E+04	3.24E+03	1.54E+00
			1729.60	3.05	2.53E+04	5.98E+03	3.18E+00
	Pb-214	0.848	74.81	6.33	2.22E+04	2.883E	2.79E+00
			77.11	10.70	2.40E+04	2.88E+03	3.02E+00
			87.20	3.70	1.25E+04	1.22E+03	1.57E+00
			295.21	19.20	7.71E+03	4.51E+02	9.71E-01
			351.92	37.20	7.58E+03	3.11E+02	9.54E-01
	Ra-226	0.989	186.21	3.28	2.93E+04	2.89E+03	3.68E+00
	Th-231	0.997	84.21	8.00	3.32E+03	6.72E+02	4.18E-01
			89.95	1.25	1.34E+04	3.72E+03	1.69E+00
	U-235	0.523	89.96	1.50	1.12E+04	3.10E+03	1.40E+00
			93.35	2.50	4.03E+04	2.88E+03	5.07E+00
			185.71	54.00	1.80E+03	1.78E+02	2.26E-01
<b>Average Dose</b>							<b>2.52E+00</b>

The average doses of the limestone samples as per the gamma spectrum analysis and nuclide identification report, there is a high correlation with respect to the doses obtained by the use of EPD and TLD. Based on the analysis of the results it can be summarized that the doses of these limestone samples are accurate and trustworthy to be used for the application of EPD in Thermo-Luminescence and Isotopic ratio dating of limestone using uranium series.

#### 4.4 ICP-MS Isotopic Ratio Results

The same samples were run on an inductively coupled plasma mass spectrometer (ICP-MS) for isotopic ratio of the uranium series nuclides and the atomic abundances for the samples are indicated in table 26 below.

**Table 26:** Atomic abundances of samples from the ICP – MS analysis

ICP-MS DATA. Mean values (n = 3)																
SAMPLE ID	Pb204	%RSD	Pb206	%RSD	Pb207	%RSD	Pb208	%RSD	U238	%RSD	U235	%RSD	U234 (x 10 <sup>-4</sup> )	%RSD	Th232	%RSD
A	0.012	0.280	0.269	0.530	0.207	0.120	0.511	0.0	0.993	0.0	0.007	2.750	1.8	3.380	1.000	0.0
B	0.012	2.040	0.267	1.130	0.208	1.180	0.512	0.0	0.993	0.0	0.007	1.550	1.6	16.860	1.000	0.0
C	0.012	1.540	0.279	0.020	0.208	0.430	0.500	0.0	0.993	0.0	0.007	2.350	1.3	7.090	1.000	0.0
D	0.013	0.940	0.277	0.210	0.210	0.050	0.501	0.0	0.993	0.0	0.007	0.340	1.4	15.790	1.000	0.0
E	0.013	1.490	0.266	0.050	0.208	0.640	0.514	0.0	0.993	0.0	0.007	1.310	1.5	19.090	1.000	0.0
F	0.013	0.670	0.266	0.420	0.207	0.380	0.514	0.0	0.993	0.0	0.007	3.260	1.8	47.020	1.000	0.0
G	0.013	1.870	0.265	0.320	0.209	0.310	0.514	0.0	0.993	0.0	0.007	0.530	1.4	4.840	1.000	0.0
H	0.013	0.110	0.264	0.520	0.209	0.310	0.514	0.0	0.993	0.0	0.007	1.860	1.2	10.830	1.000	0.0
I	0.012	1.150	0.265	0.400	0.206	0.390	0.517	0.0	0.993	0.0	0.007	0.740	2.1	3.230	1.000	0.0
J	0.012	0.250	0.264	0.110	0.207	0.630	0.517	0.0	0.993	0.0	0.007	3.840	2.2	18.350	1.000	0.0
K	0.013	1.540	0.254	0.260	0.212	0.030	0.521	0.0	0.993	0.0	0.007	1.930	1.3	8.360	1.000	0.0
L	0.013	0.470	0.253	0.120	0.214	0.590	0.520	0.0	0.993	0.0	0.007	2.750	1.4	3.540	1.000	0.0
M	0.013	1.660	0.257	1.070	0.210	0.160	0.520	0.0	0.993	0.0	0.007	0.890	1.2	1.790	1.000	0.0
N	0.013	2.930	0.256	0.810	0.212	0.700	0.520	0.0	0.993	0.0	0.007	1.260	1.2	1.190	1.000	0.0
O	0.012	2.220	0.258	1.010	0.202	0.410	0.528	0.0	0.993	0.0	0.007	6.330	0.7	128.96	1.000	0.0
P	0.012	0.270	0.259	0.580	0.203	0.090	0.527	0.0	0.993	0.0	0.007	8.490	1.5	48.280	1.000	0.0
Q	0.012	1.220	0.261	0.440	0.203	0.070	0.524	0.0	0.993	0.0	0.007	4.050	1.1	6.790	1.000	0.0
R	0.012	0.010	0.261	0.270	0.204	0.780	0.523	0.0	0.993	0.0	0.007	7.270	0.9	8.900	1.000	0.0
S	0.012	0.450	0.264	0.100	0.210	0.320	0.514	0.0	0.993	0.0	0.007	5.470	1.1	90.330	1.000	0.0
T	0.012	1.440	0.263	0.110	0.210	0.700	0.514	0.0	0.993	0.0	0.007	3.170	1.3	69.220	1.000	0.0

NWU  
LIBRARY

It is noticeable from the isotopic ratios, that the atomic abundances of  $^{234}\text{U}$  from each sample can be ignored as they are below the detection limit therefore this causes high values of %RSD for the samples. High values of %RSD as for sample P, for the isotopes  $^{235}\text{U}$  and  $^{234}\text{U}$  shows that the sample spectrums were unstable. Otherwise all the samples %RSD were within the acceptable limits (i.e. less than 3%).

Table 27, below shows the Pb isotopic ratios for each sample ID. The results obtained are in good correlation with the referenced one from the National Institute of Standards and Technology – Standard Reference Material (SRM NIST,) (<https://www.nist.gov>) opened on 10/10/2016 and are given as:

- Atomic abundance Ratio,  $^{204}\text{Pb}/^{206}\text{Pb} = 0.059042 \pm 0.000037$
- Atomic abundance Ratio,  $^{207}\text{Pb}/^{206}\text{Pb} = 0.91464 \pm 0.00033$
- Atomic abundance Ratio,  $^{208}\text{Pb}/^{206}\text{Pb} = 2.16810 \pm 0.0008$
- Atomic abundance Ratio,  $^{230}\text{Th}/^{234}\text{U} = 0.35600 \pm 0.00055$

**Table 27:** The Pb isotopic ratios for each Sample ID.

Sample ID	Measured	Measured	Measured
	<sup>208</sup> Pb/ <sup>206</sup> Pb	<sup>204</sup> Pb/ <sup>206</sup> Pb	<sup>207</sup> Pb/ <sup>206</sup> Pb
A	1.900	0.045	0.756
B	1.918	0.045	0.761
C	1.792	0.043	0.728
D	1.809	0.047	0.795
E	1.932	0.049	0.828
F	1.932	0.049	0.828
G	1.940	0.049	0.831
H	1.947	0.049	0.834
I	1.951	0.045	0.767
J	1.958	0.045	0.770
K	2.051	0.051	0.867
L	2.055	0.051	0.870
M	2.023	0.051	0.857
N	2.031	0.051	0.860
O	2.047	0.047	0.788
P	2.035	0.046	0.785
Q	2.008	0.046	0.779
R	2.004	0.046	0.779
S	1.947	0.045	0.770
T	1.954	0.046	0.773
<b>Averages</b>	1.962	0.047	0.801
<b>SDEV</b>	0.073	0.002	0.042

#### 4.5 Results for age determination due to EPD

Based on the results obtained from the methods used, calculations were done for each sample method, in order to determine the ages of the limestone samples using different age calculation formulas.

For method 1 the formula for age calculated is:

$$\text{Age} = \frac{\text{Natural Dose}}{\text{Annual Dose}}$$

**Table 28:** Ages of the EPD in TL results for the limestone sample aliquots.

Sample ID	Natural Dose (Gy)	Annual Dose (Gy/a)	Age (MY)
A	1.13E-03	3.4247E-11	33.1 ± 2.8
B	4.69E-04	4.5662E-11	10.3 ± 6.4
C	1.74E-03	4.5662E-11	38.0 ± 3.7
D	3.38E-04	3.4247E-11	9.87 ± 0.78
E	1.92E-04	4.5662E-11	4.21 ± 0.35
F	3.55E-04	3.4247E-11	10.4 ± 8.3
G	1.69E-03	2.2831E-11	74.3 ± 6.9
H	7.17E-04	3.4247E-11	20.9 ± 1.8
I	1.31E-03	5.7078E-11	23.0 ± 1.3
J	1.22E-03	6.8493E-11	17.9 ± 1.6
K	1.16E-03	4.5662E-11	25.4 ± 2.1
L	1.02E-03	9.1324E-11	11.2 ± 0.9
M	8.40E-04	3.4247E-11	24.5 ± 1.7
N	2.82E-04	9.1324E-11	3.08 ± 0.87
O	1.14E-03	2.2831E-11	50.0 ± 4.6
P	2.11E-03	6.8493E-11	30.8 ± 2.9
Q	8.08E-04	5.7078E-11	14.2 ± 1.1
R	7.69E-04	3.4247E-11	22.4 ± 1.6
S	1.38E-03	4.5662E-11	30.3 ± 2.6
T	2.69E-03	3.4247E-11	78.5 ± 6.8

From the results of EPD in TL of the limestone samples, the ages of each sample were calculated and represented in Table 28 above, having sample N with the youngest age of  $3.08 \pm 0.87$  MY and sample T with the oldest age of  $78.5 \pm 6.8$  MY. The average age for all the samples is  $26.6 \pm 1.9$  MY.

#### 4.6 Results for age determination by ICP – MS isotopic ratio technique

##### 4.6.1 Age calculation from isotopic abundances

For the ICP – MS, equation 5a and 5b below are used to calculate the ages of the samples, and the results are in table 29 below. Equation (5a) is only valid if no loss or addition of either parent or daughter nuclide occurred during the time period  $t$  (von Gunten, 1995a)



$$t = \frac{1}{\lambda_{238}} \ln \left\{ 1 + \left[ \frac{{}^{206}\text{Pb}_t - {}^{206}\text{Pb}_0}{{}^{238}\text{U}_t} \right] \right\} \quad (5a)$$

And to calculate  ${}^{206}\text{Pb}_0$  we use an approximation of (von Gunten, 1995a)

$${}^{206}\text{Pb}_0 = 5 * {}^{204}\text{Pb} \quad (5b)$$

**Table 29:** Age calculation from the isotopic ratio results for the limestone samples

Sample ID	$\lambda$	${}^{204}\text{Pb}$	${}^{206}\text{Pb}_0$	${}^{206}\text{Pb}_t$	(Ga)
A	1.55E-10	7.56E-01	3.78E+00	4.46E-02	10.99
B	1.55E-10	7.61E-01	3.81E+00	4.49E-02	20.39
C	1.55E-10	7.28E-01	3.64E+00	4.30E-02	14.91
D	1.55E-10	7.95E-01	3.97E+00	4.69E-02	20.25
E	1.55E-10	8.28E-01	4.14E+00	4.89E-02	21.68
F	1.55E-10	8.28E-01	4.14E+00	4.89E-02	27.36
G	1.55E-10	8.31E-01	4.15E+00	4.91E-02	13.47
H	1.55E-10	8.34E-01	4.17E+00	4.92E-02	18.24
I	1.55E-10	7.67E-01	3.83E+00	4.53E-02	10.83
J	1.55E-10	7.70E-01	3.85E+00	4.55E-02	20.98
K	1.55E-10	8.67E-01	4.33E+00	5.12E-02	16.91
L	1.55E-10	8.70E-01	4.35E+00	5.14E-02	12.00
M	1.55E-10	8.57E-01	4.28E+00	5.06E-02	8.44
N	1.55E-10	8.60E-01	4.30E+00	5.08E-02	6.64
O	1.55E-10	7.88E-01	3.94E+00	4.65E-02	33.49
P	1.55E-10	7.85E-01	3.92E+00	4.63E-02	27.19
Q	1.55E-10	7.79E-01	3.89E+00	4.60E-02	15.05
R	1.55E-10	7.79E-01	3.89E+00	4.60E-02	16.64
S	1.55E-10	7.70E-01	3.85E+00	4.55E-02	31.06
T	1.55E-10	7.73E-01	3.86E+00	4.56E-02	29.39

From the Isotopic ratio results it can be noted that sample N is the youngest age of  $6.6 \pm 1.2$  Ga and sample O is the oldest age of  $33.49 \pm 1.8$  Ga and the average age for all the samples being  $18.8 \pm 7.7$  Ga. There is a difference between the average ages obtained from the two methods for isotopic ratio and EPD in Thermo-Luminescence (TL) respectively. The results from the isotopic ratio technique are more consistent and more reliable. This shows that the ICP-MS Isotopic ratio technique can be used for limestone dating.

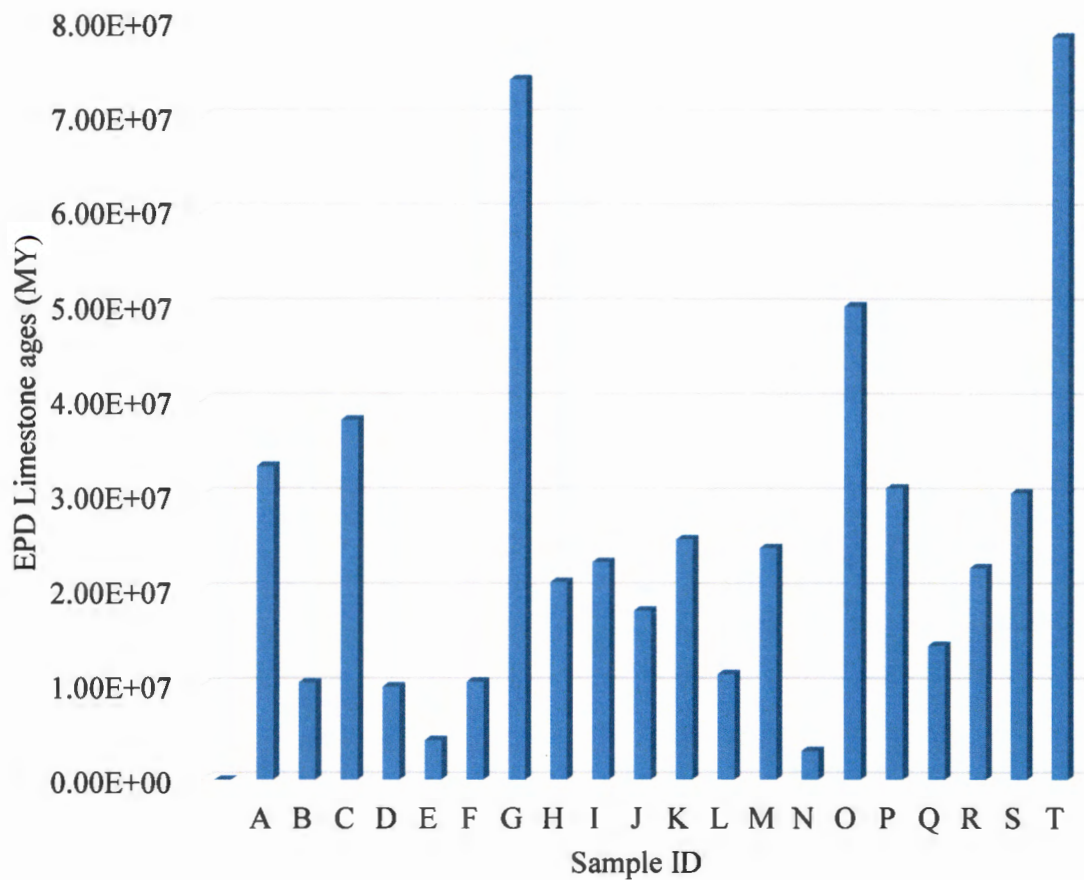


**Figure 10:** EPD dating results of limestone sample ages

It can be noted from Figure 10, that there is variance in the EPD in TL dating results of the limestones in the bar chart above, this can be due to different factors such as handling and reading of samples as well as detection by the EPD. Some of these results are comparable with the ones for isotopic ratio as some samples fall within an acceptable range with each other for both methods used.

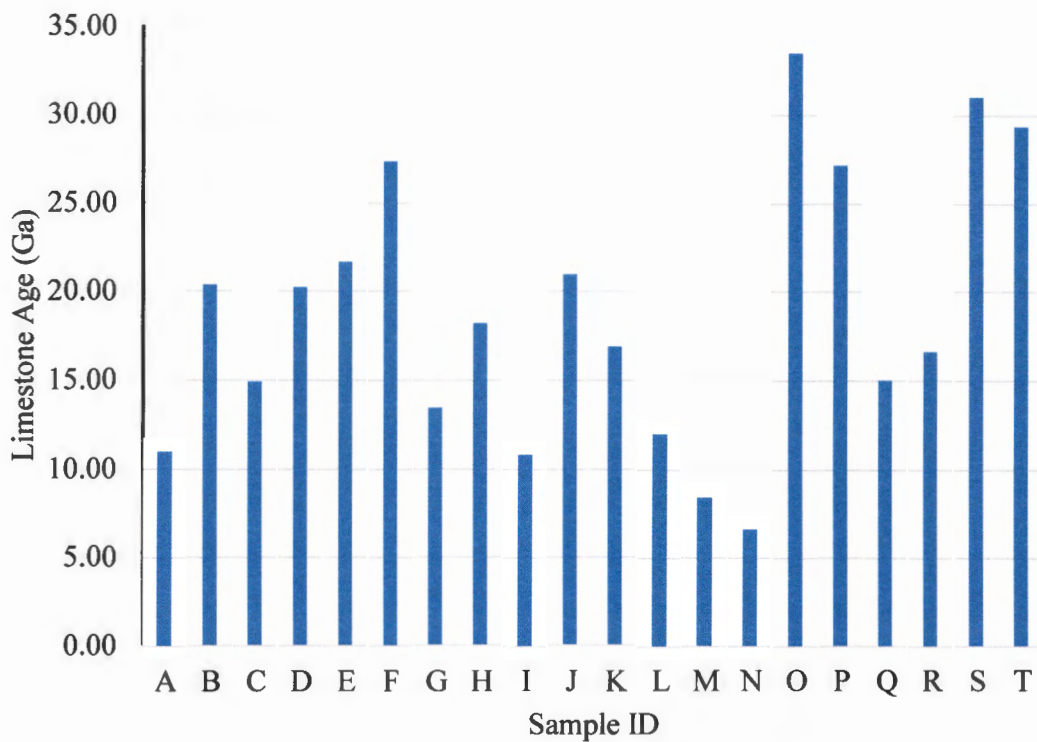


**Figure 11:** Bar chart representation of isotopic ratio dating results of limestone sample ages

The Isotopic ratios are of mutual relationship for both the samples as there is not much difference for their ages and thus gives a good analysis for how long the limestones were last exposed to heat and therefore gives a good indication of when the first settlers might have arrived and settled in Gaborone.

#### 4.6.2 U-Pb Inverse Concordia

An Isoplot Code was then conducted (Ludwig, 1998), to plot the Inverse Concordia for  $^{207}\text{Pb}/^{206}\text{Pb}$  vs  $^{238}\text{U}/^{206}\text{Pb}$  and this is shown in Figure 12 below.

**Table 30:** Concordia data for isoplot age calculations

sample ID	$^{238}\text{U}/^{206}\text{Pb}$	$^{207}\text{Pb}/^{206}\text{Pb}$
A	3.68	0.77
B	3.71	0.78
C	3.55	0.75
D	3.59	0.76
E	3.74	0.78
F	3.73	0.78
G	3.75	0.79
H	3.77	0.79
I	3.75	0.78
J	3.76	0.78
K	3.92	0.84
L	3.92	0.84
M	3.86	0.82
N	3.88	0.83
O	3.85	0.78
P	3.84	0.78
Q	3.81	0.78
R	3.81	0.78
S	3.77	0.80
T	3.77	0.80
AVER	3.77	0.79
STDEV	0.10	0.03

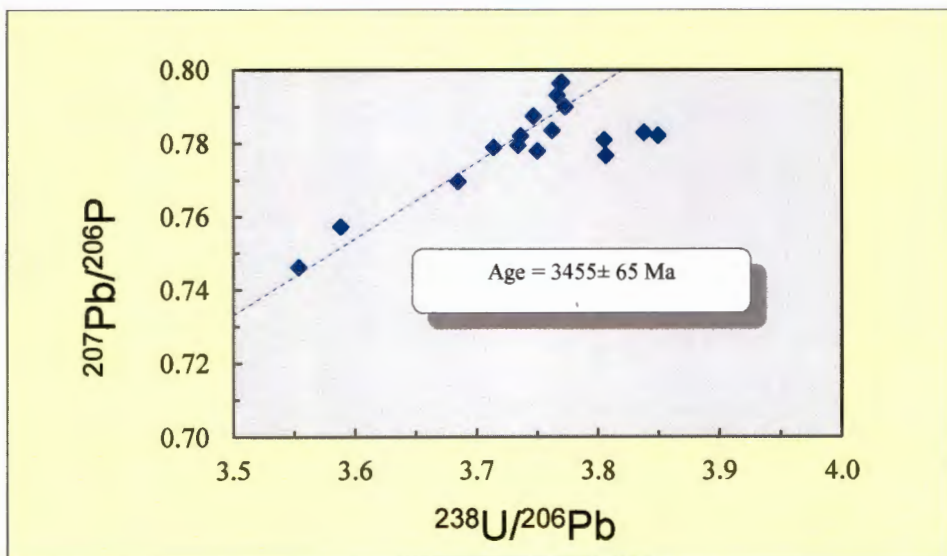


**Figure 12:** Inverse U-Pb Concordia for the limestone samples.

The results in Figure 12 above show that the average age of samples is about  $3455 \pm 65$  MY, with an MSWD of 0.15 (which reflects the goodness of the fit of the Y-X weighted mean (Ludwig, 2012)). The age given by the Isoplot from the limestone samples, of the most coherent group of 14/20 samples is 1.5 times that of SHRIMP U-Pb zircon coherent group of five samples of the Lotsane formation of the Palapye Group, from central-eastern Botswana (Mapeo et al., 2004), combines and provide a weighted mean  $^{207}\text{Pb}/^{206}\text{Pb}$  date of  $2034 \pm 8$  MY (MSWD of 0.80 and probability of 0.53) (Mapeo et al., 2004). Barton and Hallbauer (1996) argued that the age of 1860 MY which is close to that obtained by Mapeo in 2004 was too short for the time period of Black Reef ore deposit in the study area (Barton, 1996). And it is believable and evident that the age given by the U-Pb Concordia plot for the limestone samples from Gaborone area of Mogoditshane-Tsolamosese (Block 4) are more precise when bringing together ages of other geological artefacts from previous dating studies results of nearby locations.

## CHAPTER 5: CONCLUSIONS AND RECOMMENDATIONS

Gleaning from results obtained from both the methods used in the study “application of electronic personal dosimeter in Thermo-Luminescence and isotopic ratio dating of limestone using uranium series” it can be concluded that the, dating of limestone using uranium series is a possibility and it can be a precise and reliable way of dating natural and human occurrence of activities that had taken place millions year ago. These limestone dating results from Gaborone area of Mogoditshane-Tsolamosese (Block 4) will now enable the community of this area and the entire country of Botswana to be informed of how long has Gaborone geochemistry existed and also when did certain human and natural events occur, since limestone is one of the major components for human shelter construction.

From this study it can be concluded that the Gaborone area of Mogoditshane-Tsolamosese (Block 4) existed between 16 MY and 26 MY ago based on the average ages of the methods that were applied and thus all the specific objectives for this study have been met. These ages seem to be much higher than what is reported in some studies (though not Gaborone  $\approx$  500 KY) (Mercier et al., 1995). This could be reduced by moulding the dose rate variations as a function of time for burial and thus a precise knowledge of the state of disequilibrium in the Uranium decay series will be obtained for accurate luminescence (Olley et al., 1997). However the Hekpoort basalt of the Pretoria Group in Gaborone, Botswana, is reported to be  $\sim$ 2.2 GY (Yamaguchi et al., 2007). Thus the results lie in between this range.

U-Pb ages for the Ghanzi Group intersected in borehole CKP4 in northern Botswana, have been reported to be between  $1104 \pm 16$  MY, and  $1748 \pm 13$  MY on detrital zircons from the siliciclastic rocks (Kampunzu et al., 2000). Though the  $^{207}\text{Pb}/^{206}\text{Pb}$  Inverse Concordia plot from Isoplot Code gave a weighted mean age of  $4308 \pm 1900/-770$  MY for the limestone samples. The difference between zircon ages and limestone could be due to the fact that zircon are almost always buried many meters deep whereas limestone are only sampled tens of meters deep.

It is possible that when more research is done on this field of dating limestone using Uranium series by means of electronic personal dosimeter in Thermo-Luminescence and isotopic ratio more accurate and reliable database for future researcher's, scholars and historians etc. would be readily available and lingering questions on people's minds on when the first prehistoric people reside in this area will be answered whilst the future generations are ushered to a new era of sustainable dating development. Also certain natural and human activities will be able

to be dated accurately as there will be some baseline information that can be referenced to. As a recommendation, it is unmistakable that more research on dating of prehistoric activities in the country of Botswana need attention and effort for application of similar dating techniques, which will critique or upkeep the already obtained ages of historic events.

## REFERENCES

- AITKEN, M. J. 1985. *Thermoluminescence Dating*, – Standard text for introduction to the field. Quite complete and rather technical, but well written and well organized., London, Academic Press.
- BANGERT, U., FREUNDLICH J., HENNING G.J., HERR W. . 1980. Uranium series dating of calcite formations in caves: recent results and a comparative study on age determinations via Th-230/U-234, C-14, TL and ESR, In: Revue d'Archéométrie, N°4,.
- BARTON, E. S. H., D. K. 1996. Trace-element and U-Pb isotope compositions of pyrite types in the Proterozoic Black Reef, Transvaal Sequence, South Africa: Implications on genesis and ag. *Chemical Geology* 133 (1996) 133, 173-199.
- BOSNAK, C. & PRUSZKOWSKI, E. 2014. The Analysis of Drinking Waters by U.S. EPA Method 200.8 Using the NexION 300D/350D ICP-MS in Standard, Collision and Reaction Modes. *PerkinElmer, Inc. Shelton, CT*, APPLICATION BRIEF ICP - Mass Spectrometry: , 1-4.
- BOSNAK, C. A. E. P. 2014. APPLICATION BRIEF ICP - Mass Spectrometry: The Elemental Analysis of Spinach with the NexION 300/350 ICP-MS. *PerkinElmer, Inc. Shelton,, CT*: 1-4.
- CHAWLA, S. G., T.K. SINGHVI, K. 1997. QUARTZ THERMOLUMINESCENCE: DOSE AND DOSE - RATE EFFECTS AND THEIR IMPLICATIONS. *Radiation Measurements* 29, 11.
- DALRYMPLE, G. B. 2006. How Old is the Earth. A Response to "Scientific" Creationism.
- DLAMINI, S. G., MATHUTHU, M. & TSHIVHASE, V. M. 2016. Radionuclides and toxic elements transfer from the princess dump to water in Roodepoort, South Africa. *Journal of Environmental Radioactivity*, 153 201-205.
- DØSSING, L. N., FREI, R., STENDAL, H. & MAPEO, R. B. M. 2009. Characterization of enriched lithospheric mantle components in ~2.7 Ga Banded Iron Formations: An example from the Tati Greenstone Belt, Northeastern Botswana. *Precambrian Research*, 172, 334-356.
- DULLER, G. A. T. 1995. *Luminescence Dating using single aliquots methods and applications*. University of Adelaide South Australia.
- DULLER, G. A. T. & WINTLE, A. G. 2012. A review of the thermally transferred optically stimulated luminescence signal from quartz for dating sediments. *Quaternary Geochronology* 7 (2012) 6e20, 7, 6-20.
- DULLER, G. A. T. A. A. G. W. 2012. A review of the thermally transferred optically stimulated luminescence signal from quartz for dating sediments. *Quaternary Geochronology*, 7, 6-20.
- DUVAL, C., T. DEVOL AND S. HUSSON 2016. Rapid uranium isotopic analysis using ultrafiltration and alpha spectroscopy. *American Chemical Society*.
- GALLOWAY, R. B. 2003. Limestone: some observations on luminescence in the region of 360 nm. *Radiation Measurements*, 37, 177-185.
- GUIBERT, P., BECHTEL, F., SCHVOERER, M., MÜLLER, P. & BAILESCU, S. 1998. A new method for gamma dose-rate estimation of heterogeneous media in TL dating. *Radiation Measurements*, 29, 561-572.
- HORN, I., RUDNICK, R. L. & MCDONOUGH, W. F. 2000. Precise elemental and isotope ratio determination by simultaneous solution nebulization and laser ablation-ICP-MS: application to U-Pb geochronology. *Chemical Geology*, 164, 281-301.
- JACOBS, Z., WINTLE, A.G., DULLER\*G.A.T. 2003. Optical dating of dune sand from Blombos Cave, South Africa. *Journal of Human Evolution* 44 (2003)
- JOHNSON, N. M. 1960. *Thermoluminescence in biogenic calcium carbonate.*, Sedimentary Petrology
- KAMPUNZU, A. B., ARMSTRONG, R. A., MODISI, M. P. & MAPEO, R. B. M. 2000. Ion microprobe U-Pb ages on detrital zircon grains from the Ghanzi Group: implications

- for the identification of a Kibaran-age crust in northwest Botswana. *Journal of African Earth Sciences*, 30, 579-587.
- KEEGAN, E., RICHTER, S., KELLY, I. & ALONSO-MUNOZ, A. 2008. The provenance of Australian U ore concentrates by elemental and isotopic analysis. *Applied Geochemistry* 23, 765-777.
- LIN, J., LIU, Y., YANG, Y. & HU, Z. 2016. Calibration and correction of LA-ICP-MS and LA-MC-ICP-MS analyses for element contents and isotopic ratios. *Solid Earth Sciences*, 1, 5-27.
- LUDWIG, K. R. 1998. On the Treatment of Concordant Uranium-Lead Ages. *Geochimica et Cosmochimica Acta*, 62, 665-676.
- LUDWIG, K. R. 2012. User's Manual for Isoplot 3.75: . A geochronological Toolkit for Microsoft Excel. CA, USA: Berkeley Geochronology Centre.
- MANGUM, S. 2015. Uranium Isotope Ratio Measurements with the NexION ICP-MS. *Perkin Elmer Inc. Shelton, CT, APPLICATION NOTE: ICP-Mass Spectrometry*, 1-4.
- MAPEO, R. B. M., RAMOKATE, L. V., ARMSTRONG, R. A. & KAMPUNZU, A. B. 2004. U-Pb zircon age of the upper Palapye group (Botswana) and regional implications. *Journal of African Earth Sciences*, 40, 1-16.
- MCGOODWIN, M. 2010. *Geological Time (Geochronology), Summary of materials relating to course ESS 461*, University of Washington, University of Washington.
- MERCIER, N., VALLADAS, H. & VALLADAS, G. 1995. Flint thermoluminescence dates from the CFR laboratory at Gif: Contributions to the study of the chronology of the middle palaeolithic. *Quaternary Science Reviews*, 14, 351-364.
- MERCIER, N. V., H. FROGET, L. JORON, L. REYSS, L.J. WEINE, S. GOLDBERG, P. MEIGNEN, L. BAR-YOSEF, O. BELFER-COHEN, A. CHECH, M. KUHN, S.L. STINER, M.C. TILLIER, A.M. ARENSBURG, B. VANDERMEERSCH, B. 2007. Hayonim Cave: a TL-based chronology for this Levantine Mousterian sequence. *Journal of Archaeological Science* 34 (2007), 34.
- MITTELMAN, A. M. F., JOHN D.; PENNELL, KURT D. 2015. Effects of ultraviolet light on silver nanoparticle mobility and dissolution. *Environ. Sci.: Nano*, 2, 683-691
- MOFFATT, J. E., SPOONER, N.A., CREIGHTON, D.F., SMITH, B.W. 2012. Luminescence properties of common glasses for application to retrospective dosimetry. *Radiation Measurements* 47 (2012) 851e856, 47.
- NINAGAWA, K. K., T. TOYODA, S. HAYASHI, K. NISHIDO, H. KINJO, M. KAWANA, T. 2001. Thermoluminescence dating of the Ryukyu Limestones. *Quaternary Science Reviews* 20 (2001) 829}833, 20, 5.
- OLLEY, J. M., ROBERTS, R. G. & MURRAY, A. S. 1997. Disequilibria in the uranium decay series in sedimentary deposits at Allen's cave, nullarbor plain, Australia: Implications for dose rate determinations. *Radiation Measurements*, 27, 433-443.
- PRESCOTT, J. R. & HUTTON, J. T. 1995. Environmental dose rates and radioactive disequilibrium from some Australian luminescence dating sites. *Quaternary Science Reviews*, 14, 439-448.
- REYNOLDS, C. 2015. The Thorium SVG image by Wikipedia contributor BatesIsBack and the Radium Series png image Wikipedia contributor Tosaka.
- RICHTER, D. 2007. Advantages and Limitations of Thermoluminescence Dating of Heated Flint from Paleolithic Sites. *Geoarchaeology: An International Journal*, , , Vol. 22, No. 6, 671 - 683.
- ROQUE, C. G., P. VARTANIAN E. BECHTEL, F. SCHVOERER, M. 2001. Thermoluminescence \* dating of calcite: study of heated limestone fragments from Upper Paleolithic layers at Combe Saunie`re, Dordogne, France. *Quaternary Science Reviews* 20 (2001) 935}938, 20, 4.
- STANFORD, N. 2009. Dosimetry. Stanford Dosimetry: Stanford Dosimetry.
- STANLEY, F. E. 2012. A beginner's guide to uranium chronometry in nuclear forensics and safeguards. *J. Anal. At. Spectrom* 27, 1821 - 1830.

- THIRLWALL, M. F. & ANCZKIEWICZ, R. 2004. Multidynamic isotope ratio analysis using MC-ICP-MS and the causes of secular drift in Hf, Nd and Pb isotope ratios. *International Journal of Mass Spectrometry*, 235, 59-81.
- VERNI, E. R. L., AGUSTÍN, BAZÁNA, CRISTIAN; STRASSER, EDGARDO; PERINO, ERNESTO; GIL, RAÚL A. 2017. REE profiling in basic volcanic rocks after ultrasonic sample treatment and ICPMS analysis with oxide ion formation in ICP enriched with O<sub>2</sub>. *Microchemical Journal* 130, 14–20.
- VILTA, M. 2016. *NexION 300 ICP-MS Instruments Animation* [Online]. Perkin Elmer Inc. Shelton, CT. Available: <https://www.youtube.com/watch?v=L-FYh2z9mi0> [Accessed 15 November 2016 2016].
- VON GUNTEN, H. R. 1995a. Radioactivity: A Tool to Explore the Past. *Radiochimica Acta* 70/71, (1995), 70, 305 - 316.
- VON GUNTEN, H. R. 1995b. *Radioactivity: A Tool to Explore the Past*. Paul Scherrer Institut, CH-5232 Vilhigen PSI.
- YAMAGUCHI, K. E., JOHNSON, C. M., BEARD, B. L., BEUKES, N. J., GUTZMER, J. & OHMOTO, H. 2007. Isotopic evidence for iron mobilization during Paleoproterozoic lateritization of the Hekpoort paleosol profile from Gaborone, Botswana. *Earth and Planetary Science Letters*, 256, 577-587.
- YIP, Y.-C., J. C.-W. LAM AND W.-F. TONG 2008. Applications of lead isotope ratio measurements. *Trends in Analytical Chemistry*, 27, 20.
- YIP, Y.-C., LAM, J. C.-W. & TONG, W.-F. 2008. Applications of lead isotope ratio measurements. *Trends in Analytical Chemistry*, Vol. 27, No. 5, 2008, 27, 460-480.

**Appendix A: List of publications from this work**

1. Tshogfatso W Solomon and **Manny Mathuthu**. Application of Electronic Personal Dosimeter in Thermo-Luminescence and Isotopic Ratio (Radiometric) Dating of Limestone Using Uranium Series. *Imperial Journal of Interdisciplinary Research*. **Vol. 3, (3)**. (*accepted March 2017*)